References

1. Zipes DP. The long QT interval syndrome. A Rosetta stone for sympathetic related ventricular tachyarrhythmias. Circulation 1991;84:1414-1419.
2. Curran ME, Splawski I, Timothy KW, Vincent GM, Green ED, Keating MT. A molecular basis for cardiac arrhythmia: HERG mutations cause long QT syndrome. Cell 1995;80:795-803.
3. Wang Q, Shen J, Splawski I, et al. SCN5A mutations associated with an inherited cardiac arrhythmia, long QT syndrome. Cell 1995;80:805-811.
4. Morita H, Wu J, Zipes DP. The QT syndromes: long and short. Lancet 2008;372:750-763.
5. Ackerman MJ. The long QT syndrome: ion channel diseases of the heart. Mayo Clinic proceedings Mayo Clinic 1998;73:250-269.
6. Schulze-Bahr E, Wang Q, Wedekind H, et al. KCNE1 mutations cause jervell and Lange-Nielsen syndrome. Nature Genetics 1997;17:267-268.
7. Ackerman MJ, Mohler PJ. Defining a new paradigm for human arrhythmia syndromes: phenotypic manifestations of gene mutations in ion channel- and transporter-associated proteins. Circulation Research 2010;107:457-465.
8. Chen L, Carroll SJ, Kurokawa J, Kass RS. KCNQ1/KCNE1 macromolecular signaling complex: channel microdomains and human disease. In: Zipes DP, Jalife J, eds. Cardiac Electrophysiology: From cell to bedside, 5th ed. 5th ed. Philadelphia: SAUNDERS, ELSEVIER; 2009:187-194.
9. Nakajo K, Kubo Y. Nano-environmental changes by KCNE proteins modify KCNQ channel function. Channels (Austin) 2011;5:397-401.
10. Lundby A, Tseng GN, Schmitt N. Structural basis for K(V)7.1-KCNE(x) interactions in the I(Ks) channel complex. Heart rhythm 2010;7:708-713.
11. Xu X, Jiang M, Hsu KL, Zhang M, Tseng GN. KCNQ1 and KCNE1 in the IKs channel complex make state-dependent contacts in their

extracellular domains. The Journal of General Physiology 2008;131:589-603.

12. Kang C, Tian C, Sonnichsen FD, et al. Structure of KCNE1 and implications for how it modulates the KCNQ1 potassium channel. Biochemistry 2008;47:7999-8006.
13. Wrobel E, Tapken D, Seebohm G. The KCNE Tango - How KCNE1 Interacts with Kv7.1. Frontiers in Pharmacology 2012;3:142.
14. Choi SH, Shin TJ, Lee BH, et al. Ginsenoside Rg3 activates human KCNQ1 K+ channel currents through interacting with the K318 and V319 residues: a role of KCNE1 subunit. European Journal of Pharmacology 2010;637:138-147.
15. Lvov A, Gage SD, Berrios VM, Kobertz WR. Identification of a protein-protein interaction between KCNE1 and the activation gate machinery of KCNQ1. The Journal of General Physiology 2010;135:607-618.
16. Zheng R, Thompson K, Obeng-Gyimah E, et al. Analysis of the interactions between the C-terminal cytoplasmic domains of KCNQ1 and KCNE1 channel subunits. The Biochemical Journal 2010;428:75-84.
17. Choveau FS, Rodriguez N, Abderemane Ali F, et al. KCNQ1 channels voltage dependence through a voltage-dependent binding of the S4-S5 linker to the pore domain. The Journal of Biological Chemistry 2011;286:707-716.
18. Girmatsion Z, Biliczki P, Takac I, Schwerthelm C, Hohnloser SH, Ehrlich JR. N-terminal arginines modulate plasma-membrane localization of Kv7.1/KCNE1 channel complexes. PloS One 2011;6:e26967.
19. Labro AJ, Boulet IR, Choveau FS, et al. The S4-S5 linker of KCNQ1 channels forms a structural scaffold with the S6 segment controlling gate closure. The Journal of Biological Chemistry 2011;286:717-725.
20. Hoosien M, Ahearn ME, Myerburg R, J., et al. Dysfunctional potassium channel subuinit interaction as a novel mechanism of long QT syndrome. Heart Rhythm 2013;10:in press.

Journal of Arrhythmia ▮ (▮▮▮▮) ▮▮▮–▮▮▮

Contents lists available at SciVerse ScienceDirect

Journal of Arrhythmia

journal homepage: www.elsevier.com/locate/joa

Clinical outcome and risk stratification in Brugada syndrome

Tadashi Wada, MD[1], Hiroshi Morita, MD*[2], PhD

Department of Cardiovascular Medicine, Okayama University Graduate School of Medicine, Dentistry and Pharmaceutical Sciences, Okayama, Japan

2 Department of Cardiovascular Therapeutics, Okayama University Graduate School of Medicine, Dentistry and Pharmaceutical Sciences, Okayama, Japan

ARTICLE INFO

Article history:
Received 26 November 2012
Received in revised form
29 November 2012
Accepted 4 December 2012

Keywords:
Brugada syndrome
Ventricular fibrillation
Risk stratification
ECG

ABSTRACT

Since the first report on Brugada syndrome, various risk markers for the prediction of ventricular fibrillation (VF) in patients with Brugada syndrome have been reported. Multicenter trials reported spontaneous type 1 electrocardiogram (ECG) and disease symptoms as prognostic predictors. VF induction by programmed electrical stimulation is still controversial, and most of the studies have failed to prove its significance for the prediction of spontaneous VF episodes. In Japan, although most multicenter studies have shown that patients with type 1 ECG were at high risk, it is difficult to determine the indication for implantation of an implantable cardioverter defibrillator only based on the ECG type. Recent studies have added new risk markers, such as inferolateral early repolarization, fragmented QRS, and shorter effective refractory periods of the ventricle, in addition to type 1 ECG and symptoms. Here, we review the clinical outcome and indices reported as reliable prognostic factors of Brugada syndrome with a focus on the clinical and ECG markers for risk stratification.

Contents

1. Introduction 2
   1.1. Long-term prognosis of Brugada syndrome 2
2. Clinical characteristics and prognosis 3
   2.1. Symptoms 3
   2.2. Family history of sudden death and SCN5A mutation 3
   2.3. Gender difference and children 3
3. Repolarization abnormality and prognosis 4
   3.1. Type 1 ECG and prognosis 4
   3.2. Non-type 1 ECGs 4
   3.3. Alternation in ST-T segment 4
   3.4. Abnormality in QT intervals 4
   3.5. Physiologic provocation test to unmask type 1 ECG 4
   3.6. Inferolateral early repolarization 5
4. Depolarization abnormality and prognosis 6
   4.1. QRS interval and axis 6
   4.2. Fragmented QRS complex 7
   4.3. Prolongation of the PQ interval 7
   4.4. Signal-averaged electrogram 7
5. Other indices 7
   5.1. Prediction of outcome by electrophysiological study 7
   5.2. Atrial arrhythmias 7
6. Summary and proposed risk stratification 8
Conflict of interest 8
Acknowledgments 8
References 8

* Correspondence to: Department of Cardiovascular Therapeutics, Okayama University Graduate School of Medicine and Dentistry, 2-5-1 Shikata-Cho, Okayama City, Okayama 700-8558, Japan. Tel.: +81 86 235 7351; fax: +81 86 235 7353.
E-mail address: hmorita@cc.okayama-u.ac.jp (H. Morita).

1880-4276/$ - see front matter © 2013 Japanese Heart Rhythm Society. Published by Elsevier B.V. All rights reserved.
http://dx.doi.org/10.1016/j.joa.2012.12.008

Please cite this article as: Wada T, Morita H. Clinical outcome and risk stratification in Brugada syndrome. J Arrhythmia (2013), http://dx.doi.org/10.1016/j.joa.2012.12.008

1. Introduction

Twenty years have passed since the first report on Brugada syndrome [1]. The interesting electrocardiogram (ECG) characteristics of this syndrome have attracted the attention of many physicians and researchers, and almost 2000 reports on Brugada syndrome have been published. Symptomatic patients who have had a previous episode of aborted cardiac arrest (ACA) and syncope are at high risk for recurrent ventricular tachyarrhythmias. Previous studies that evaluated the long-term prognosis of Brugada syndrome patients have shown that a previous episode of ACA and syncope are high-risk markers [1–5]. Some studies have also shown various clinical risk factors for identifying high-risk patients (Table 1). Most of the observations from which risk factors for ventricular fibrillation (VF) were identified were carried out in patients who experienced cardiac arrest or VF, and it is still not clear whether these risk factors can identify high-risk patients among those in whom VF has not been documented.

Here, we review the clinical outcome and indices reported as reliable prognostic factors of Brugada syndrome with a focus on the clinical and ECG markers for risk stratification.

1.1. Long-term prognosis of Brugada syndrome

Brugada et al. [6] published the first report on the long-term prognosis of patients with Brugada syndrome. They followed 63 patients (including 22 asymptomatic patients) for 34 months and found a high incidence of cardiac events (~30% during follow-up) regardless of the presence or absence of symptoms. Subsequent studies showed relatively lower incidences of VF events, especially in patients without documented VF, and recent studies have shown that the event rates were 0.5–1% per year in asymptomatic patients and 0.6–3.4% per year in patients with syncope [3–5].

Table 1
Risk markers reported in Brugada syndrome.

Clinical characteristics	ECG markers	Additional examination
Male	Repolarization abnormality	Signal-averaged electrogram
Syncope	Spontaneous type 1 ECG	Late potential
Family history of sudden death	ST level (V2)	
	ST augmentation after exercise	Antiarrhythmic drug test
	ST augmentation after meal/full stomach/glucose	Pilsicainide-induced TWA, VT
	QT prolongation, longer T_{peak}–T_{end}	
	Inferolateral early repolarization	Electrophysiological study
	Spontaneous alteration of ST level/ECG types	PES-induced VF
	T wave alternans (macroscopic)	
	Negative T wave (V1)	Mode of induction
	Depolarization abnormality	ERP < 200 ms
	PQ prolongation	
	Fragmented QRS	
	QRS widening	
	aVR sign	
	Arrhythmias	
	Atrial fibrillation/SSS/AV block	

Table 2
Long-term prognosis in Brugada syndrome.

	Brugada [6]	Priori 2000	Atarashi 2001	Brugada 2002 [2]	Brugada 2003	Eckardt 2005	Takagi 2007 [67]	Kamakura 2009 [5]	Probst [3] (FINGER registry)	Priori [4] (PRELUDE registry)
Number of pts	63	60	105	334	547	212	188	330	1029	308
Age (years)	38 ± 17	40 ± 15	45 ± 13	42 ± 16	41 ± 15	45 ± 6	53 ± 14	51 ± 19	45 (35 to 55)	47 ± 12
Follow-up (months)	34 ± 32	33 ± 38	36	33 ± 39	24 ± 32	40 ± 50	37 ± 16	49 ± 15	32 (14 to 54)	36 ± 8
Male (%)	90	75	94	76	75	72	95	95	72	80
Symptoms (%)										
Asymptomatic	35	50	64	57	77	58	52	63	64	79
Syncope	32	22	17	22	23	31	26	20	30	21
VF	33	28	19	21	0	11	22	17	6	0
Induced VF (%)	80 (37/46)	67 (26/39)	NA	52 (130/252)	40 (163/408)	50 (93/186)	78 (114/146)	59 (138/232)	41 (262/638)	41 (126/308)
VF event rate (%/yr)										
Asymptomatic pts	12	0	0.5	3.5	1.5*	0.2	0	0.5	0.5	1
Pts with syncope	18	4	8.6	8.8	7.0*	1.8	1.9	0.6	1.9	3.6
Pts with VF	11			13.8	–	5.1	9.8	10.2	7.7	-
Predictors										
ECG	–	–	–	Spont. type 1 ECG	Spont. type 1 ECG	Spont. type 1 ECG	rJ (V2) ≥ 90 ms QRS (V6) ≥ 90 ms	Inferolateral ER	Spont. type 1 ECG	QRS fragmentation
Symptom	–	–	–	–	Syncope	ACA / syncope	–	Family history of SD < 45 years	Syncope	Syncope
EPS	–	–	–	Induced VT/VF	Induced VT/VF	–	–	–	–	ERP < 200 ms

Please cite this article as: Wada T, Morita H. Clinical outcome and risk stratification in Brugada syndrome. J Arrhythmia (2013), http://dx.doi.org/10.1016/j.joa.2012.12.008

Patients with previously documented VF still had high event rates (7.7–10.2% per year) in recent studies [2,3,5,7] (Table 2, Fig. 1). These studies proved that the spontaneous appearance of type 1 ECG, syncope, and ACA were high-risk markers for VF events during follow-up. Prospective studies carried out in the past 3 years added the existence of inferolateral early repolarization (ER) and QRS fragmentation to the risk markers predicting VF events [4,5]. The value of VF induction by programmed electrical stimulation for risk stratification in Brugada syndrome was controversial [8–10]; however, meta-analyses of the results of VF induction failed to prove the usefulness of induced VF for risk stratification [11,12].

On the basis of a meta-analysis involving 1545 patients performed in 2006, it was concluded that a history of syncope or aborted sudden cardiac death (SCD) (relative risk [RR], 5.51), spontaneous type 1 ECG (RR, 4.65), and male gender (RR, 4.47) can predict the prognosis of patients; however, family history of sudden death, sodium channel gene (*SCN5A*) mutation, and programmed stimulation cannot predict the subsequent occurrence of VF [11].

2. Clinical characteristics and prognosis

2.1. Symptoms

A previous episode of ACA is a high-risk marker of VF recurrence during follow-up (hazard ratio [HR], 11) [3]. Therefore, implantation of an implantable cardioverter defibrillator (ICD) should be recommended for the secondary prevention of SCD [13]. It is also acceptable to implant an ICD in patients with documented ventricular tachycardia (VT) not resulting in aborted SCD.

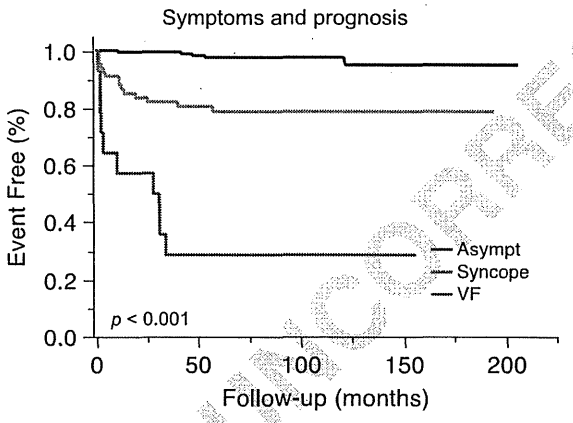

Fig. 1. Prognosis of Brugada syndrome according to symptoms. Asymptomatic patients had good prognosis; however, the event rates increased in patients with syncope and ventricular fibrillation. Data from 250 patients (asymptomatic, 170 patients; syncope, 67 patients; aborted cardiac arrest, 17 patients).

An episode of syncope is a sensitive predictor of sudden cardiac arrest in patients with Brugada syndrome (HR, 2.5–6.4) [3,4,7,14]. Recording of a spontaneous or a drug-induced type 1 ECG is important for detecting high-risk patients among those who have had syncope episodes [15]. Indeed, 20% of sudden death cases caused by this syndrome had at least 1 syncope episode before the fatal event [16]. However, not all syncope episodes occur from VF, and syncope can also occur from bradyarrhythmias, neutrally mediated syncope, and epileptic seizures [17,18]. An extracardiac cause of syncope should be excluded at the time of diagnosis; however, it is sometimes difficult to prove that a patient's symptoms have not resulted from VF unless an ECG is recorded during the episode itself. Then, it is important to evaluate the circumstances and the existence of a prodrome at the onset of the syncope episode [19]. Recently, we reported that syncope episodes with prodromes, especially symptoms such as blurred vision (HR, 0.20), diaphoresis, and symptoms related to urination, are less frequently associated with VF episodes and may be associated with benign episodes. In contrast to these symptoms, the absence of these prodromes and abnormal respiration at night (HR, 2.39) are independently associated with VF episodes [20].

2.2. Family history of sudden death and SCN5A mutation

Although most of the European studies failed to prove an association between family history of sudden death and VF events [3,4,7,21], frequent sudden deaths in family members were recognized [22]. A Japanese registry proved that a family history of sudden death (< 45 years) was an independent predictor of subsequent VF events (HR, 3.28) [5].

In most series, there was no difference in arrhythmic events according to the presence or absence of mutations of the cardiac sodium channel gene (*SCN5A*) [3,11,14]. Some studies have shown a significantly higher rate of recurrent VF among patients carrying *SCN5A* mutations [23] and loss-of-function mutations, compared with patients without such mutations [24]. Mutations associated with calcium and potassium channels and the β-subunit of the sodium channel are rare [25], and the impact of these mutations on prognosis is unclear.

2.3. Gender difference and children

It is well known that Brugada syndrome has a male predominance (~80%) [26]. In an experimental model of Brugada syndrome, male canines have been shown to frequently have the Brugada

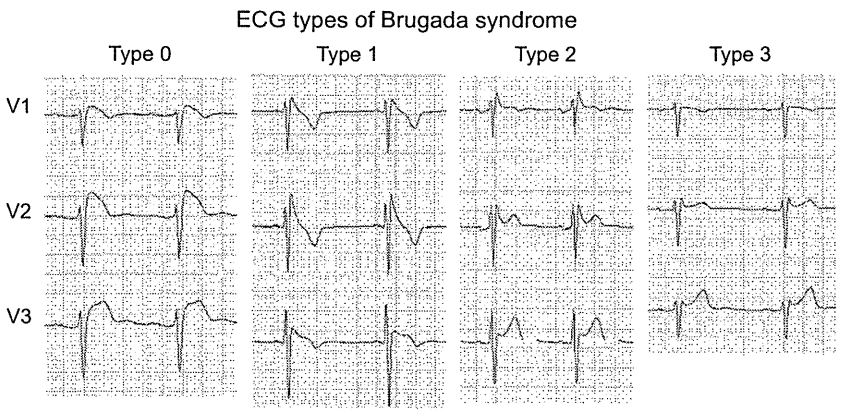

Fig. 2. ECG types of Brugada syndrome.

Please cite this article as: Wada T, Morita H. Clinical outcome and risk stratification in Brugada syndrome. J Arrhythmia (2013), http://dx.doi.org/10.1016/j.joa.2012.12.008

phenotype [27] and androgen has been shown to be important for the development of this syndrome [28,29]. Men had greater rates of spontaneous type 1 ECG, greater ST-segment elevation, and greater inducibility of VF than women. Male gender was significantly related to cardiac events during follow-up (HR, 4.45) [11,21,30].

Spontaneous VF or sudden death usually occurs at middle age [31], and Brugada-type ECG in children is very rare. The prevalence of Brugada-type ECG in children has been reported to be 0.005–0.0098% [32,33], and it increases up to puberty. Although its incidence is low, children with Brugada syndrome can show severe clinical forms [1,34]. Severe infant cases have also been reported and are associated with conduction abnormality. Syncope episodes in children are frequently precipitated by fever [34].

3. Repolarization abnormality and prognosis

3.1. Type 1 ECG and prognosis

The diagnosis of Brugada syndrome requires the existence of type 1 ECGs. Report of the Second Consensus conference stated that type 1 ECG is only diagnostic of Brugada syndrome and is defined by a coved ST-segment elevation of ≥ 2 mm (0.2 mV) followed by a negative T wave (Fig. 2). The criteria for the diagnosis of Brugada syndrome are the existence of type 1 ECG in the presence or absence of a sodium channel blocker and VF/VF (spontaneous or induced), symptoms (syncope or agonal respiration), and family history of sudden death [13]. Type 1 ECG has been identified as an independent predictor of ventricular tachyarrhythmias in multivariate analyses of the largest cohorts of patients [2,3,14,35]. The HR of spontaneous type 1 ECG was reported [3] to be 1.8, and it increases when it is combined with the patient's symptom (syncope) (HR, 4.2–6.4) [7,14].

Type 1 ECG is usually prominent in lead V2 [36], especially at high intercostal spaces (ICSs) [37,38]. If patients only have type 1 ECG at leads V1 and V2 of the 2nd or 3rd ICS and do not show typical ECG in standard lead locations, the prognosis of the patients is similar to that of patients with a type 1 ECG in standard leads V1 and V2 [39]. This observation indicates that detection of type 1 ECG is important irrespective of the location of leads V1 and V2. Type 1 ECG at lead V2 represents abnormal repolarization at the right ventricular outflow tract (RVOT), and a variation in the relative location between the RVOT and lead V2 will cause different appearances of typical Brugada-type ECG at the 2nd to 4th ICSs [40].

Experimental observations have shown that VF occurs when the morphology of the epicardial action potentials (APs) changes functionally and results in prominent heterogeneity of APs within the epicardium. These arrhythmogenic AP changes are accompanied by ECG morphology changes from type 1 ECG to coved-type ST elevation with shallowing of the negative T wave or without negative T waves [41]. Take et al. defined this type as "type 0 ECG" and found that it frequently appeared in association with VF episodes (Fig. 2).

3.2. Non-type 1 ECGs

Patients with type 2 and 3 ECGs are thought to have a more benign clinical course compared with patients with spontaneous type 1 ECGs. In the Consensus reports, these ECG types were defined as saddleback-type ST segment (≥ 2 mm) with a positive or biphasic T wave (type 2) and a saddleback or coved-type ST segment of < 1 mm (type 3) [13], and these types are considered non-diagnostic ECG.

From the experimental model of Brugada syndrome, these ECG types represent less arrhythmogenic abnormality of repolarization [42]. However, not all patients without spontaneous type 1 ECG have good prognosis. Indeed, patients without spontaneous type 1 ECG who have experienced ACA had a recurrence of VF during follow-up [5]. Administration of a sodium channel blocker is used to unmask type 1 ECG from non-type 1 ECGs, and it can identify high-risk patients among those with non-type 1 ECGs. The prognosis for patients with drug-induced type 1 ECG is worse than that for patients without such ECG manifestations [43]. A recent study showed that the response to sodium channel blocker can be predicted by measurement of the angle of the late r′ wave (angle between the upstroke of the S wave and downslope of the r′ wave) [44]. Patients with drug-induced type 1 ECG had a blunter r′ wave than did patients without such ECGs, and the cutoff value was 58° (Fig. 3).

3.3. Alternation in ST-T segment

T-wave alternans (TWA) represents an unstable repolarization process and is often observed in patients with long QT syndrome. Unstable repolarization promotes heterogeneity of APs and initiates ventricular arrhythmia. A Brugada syndrome model showed the instability of the epicardial AP in the RVOT that resulted in macroscopic TWA and promoted ventricular arrhythmias [42,45]. In patients with Brugada syndrome, macroscopic TWA occurred as beat-by-beat alternans of the negative T wave and ST elevation (Fig. 4A) and appeared in association with syncope episodes [46], fever [47], administration of antiarrhythmic drug [48], and glucose tolerance test [49]. Antiarrhythmic drug-induced TWA was frequently observed in patients with spontaneous VF [50]. Macroscopic TWA is associated with VF; however, microvolt TWA induced by exercise did not predict the occurrence of VF [51].

Although TWA occurred as a very short-term instability of repolarization, patients also showed long-term ST-T variations (Fig. 4B). The ST level is augmented especially in association with VF episodes [52]. These ECG variations were termed ECG fluctuations [53] or alterations [41]. The ECG type in a patient can alternate between types 1, 2, 3, and normal ECGs even if a typical spontaneous type 1 ECG has been recorded. Patients who had frequent appearances of type 1 ECG had more appropriate ICD shocks [54] and VF induction by programmed stimulation [53]. ECG type alteration and ST level variations of ≥ 0.20 mV were independently associated with VF [41]. These indices of TWA and ST alteration were evaluated in a small number of patients (< 100) and have not been tested in a randomized trial.

3.4. Abnormality in QT intervals

Some studies have analyzed abnormal QT intervals in patients with Brugada syndrome, although they included small numbers of patients. One study showed that a long QT interval in lead V2 (QTc > 460 ms) and a long T_{peak}–T_{end} interval were associated with VF events [55]. Moreover, the response of QT interval to RR interval change is deteriorated in patients with VF [56]. Deep negative T wave in lead V1 (< -105 μV) is also associated with poor prognosis during follow-up (odds ratio [OR], 8.98) [57]. These abnormalities in QT-T segments may represent abnormal repolarization processes in the ventricle.

3.5. Physiologic provocation test to unmask type 1 ECG

The diagnostic type 1 ST-segment elevation is highly variable over time and is often absent in affected individuals [41,53]. An antiarrhythmic drug test with a sodium channel blocker is widely used to unmask type 1 ECG. Some physiological provocation tests for stratifying the risk of patients have been proposed.

Please cite this article as: Wada T, Morita H. Clinical outcome and risk stratification in Brugada syndrome. J Arrhythmia (2013), http://dx.doi.org/10.1016/j.joa.2012.12.008

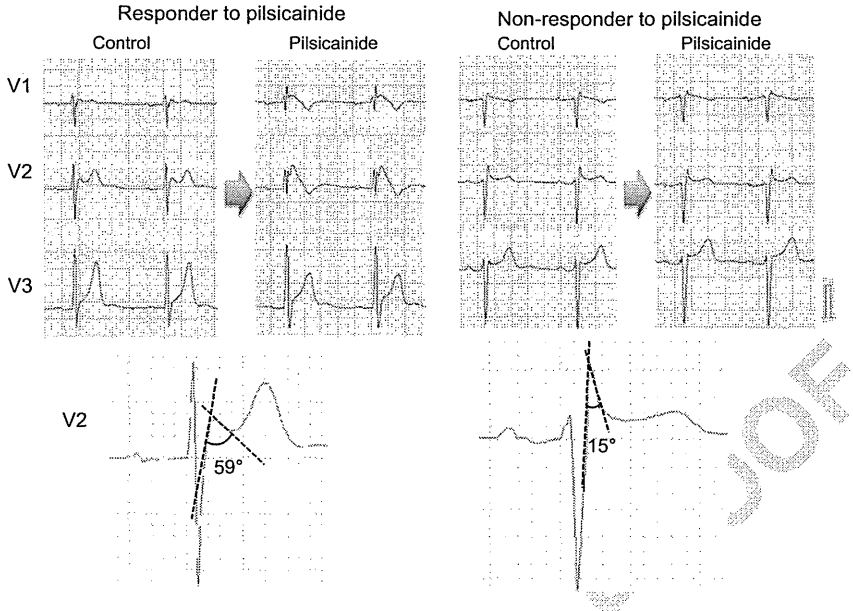

Fig. 3. Response to pilsicainide in patients with non-type 1 ECG. Pilsicainide induced ST elevation in a patient with a large degree of late r′ wave (left). Patients with a sharp degree of r′ wave did not respond to pilsicainide.

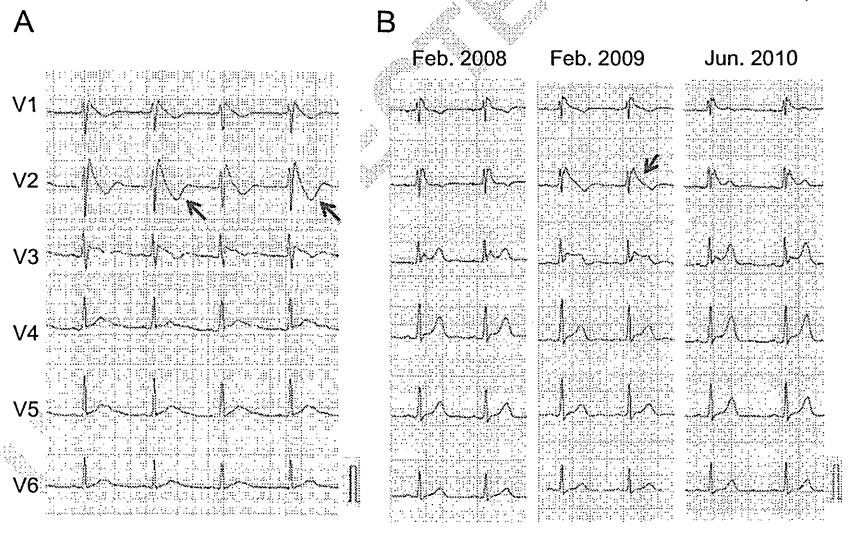

Fig. 4. T-wave alterations. (A) T-wave alternans in a patient with ventricular fibrillation. Arrows show the beat-by-beat changes of the negative T wave. (B) Spontaneous ST alteration in an asymptomatic patient. This patient had type 2 or 3 ECGs, but type 1 ECG appeared spontaneously in February 2009.

Sympathetic nerve stimulation reduces ST elevation, and a stormy occurrence of VF events can be terminated by the administration of a β-adrenergic stimulant. However, some patients have augmented ST elevation at the recovery phase of an exercise test in which the vagal nerve activity may increase. Makimoto et al. [58] reported that ST-segment augmentation at early recovery during exercise testing was observed in a third of patients and was an independent predictor for VF during follow-up periods (HR, 3.17) (Fig. 5).

The ST level is augmented by the intake of glucose or a meal in patients with Brugada syndrome [59–61]. A full stomach test by intake of a large meal within 20 min at lunch augmented ST elevation in high-risk patients with Brugada syndrome [62] (OR, 7.1). The ST augmentation after meals will cause the occurrence of ACA at night and after dinner during high vagal nerve activity.

3.6. *Inferolateral early repolarization*

Several studies have suggested an association of idiopathic VF with ER or J wave [63]. Recently, inferolateral ER has been defined as an elevation of the J point (≥ 0.1 mV) in at least two leads and includes QRS slurring or notching in inferior leads (II, III, and aVF), lateral leads (I, aVL, and V4–V6), or both [5,63]. An ER pattern in inferolateral leads is not rare in patients with Brugada syndrome (Fig. 6), and its incidence was 11–12% [5,64,65]. This pattern of ST elevation was not enhanced by an antiarrhythmic drug test [65,66] but was frequently associated with VF or syncope episodes [5,65]. Kamakura et al. [5,65] demonstrated that inferolateral ER in patients with spontaneous type 1 ECG was an independent predictor of a fatal arrhythmic event (HR, 3.28), whereas Letsas et al. [64] did not find any significant difference in the analysis of ER in Brugada syndrome.

Please cite this article as: Wada T, Morita H. Clinical outcome and risk stratification in Brugada syndrome. J Arrhythmia (2013), http://dx.doi.org/10.1016/j.joa.2012.12.008

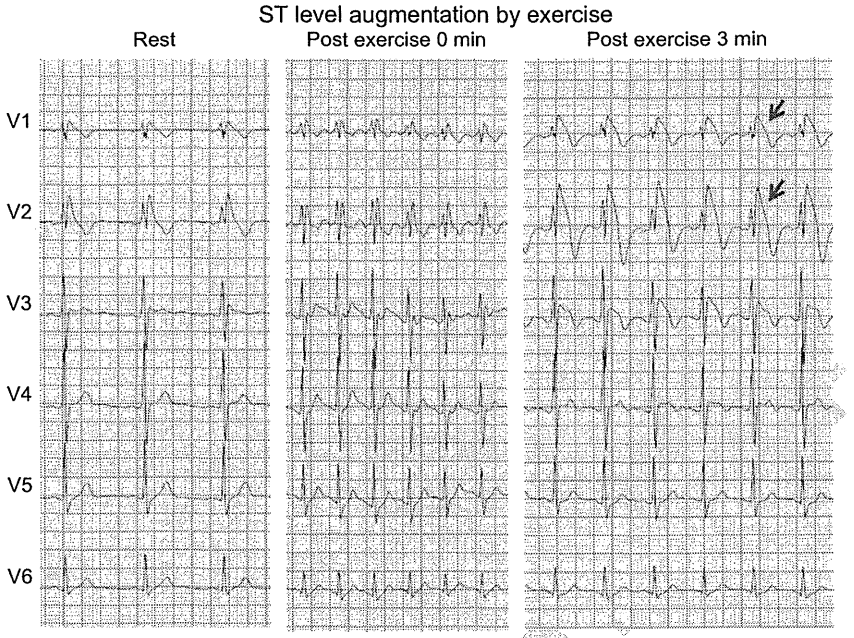

Fig. 5. ST level augmentation by exercise. ST level increased and a typical type 1 ECG appeared after exercise.

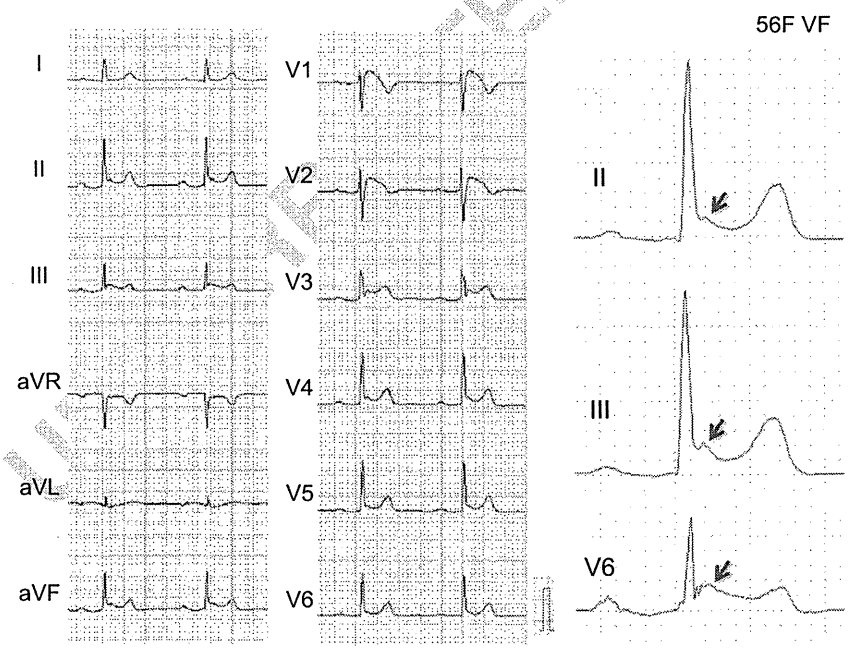

Fig. 6. Inferolateral early repolarization. This patient with spontaneous ventricular fibrillation (VF) had type 1 ECG and inferolateral early repolarization (arrows).

4. Depolarization abnormality and prognosis

4.1. QRS interval and axis

It has been reported that a wide QRS complex is associated with the occurrence of VF. Patients with VF often have a wide QRS complex and S wave. An S wave width of ≥ 80 ms in lead V1 has a high sensitivity and specificity for patients with VF [36]. The usefulness of a wide QRS complex for VF prediction was proved by two studies that included a large number of patients. Takagi et al. [67] evaluated the QRS interval in the right precordial leads as the "rJ interval," and found that an rJ interval (V2) of ≥ 90 ms and a QRS interval (V6) of ≥ 90 ms were possible predictors of the recurrence of cardiac events in symptomatic patients. A subsequent study also showed that symptomatic patients had a wider QRS complex (V2, 115 ± 26 ms) than did asymptomatic patients (104 ± 19 ms), and that the optimized cutoff point of V2 QRS of ≥ 120 ms gave an OR of 2.5 for being symptomatic [68].

The axis of the QRS complex often becomes leftward in direction in patients with Brugada syndrome. A study with a

Please cite this article as: Wada T, Morita H. Clinical outcome and risk stratification in Brugada syndrome. J Arrhythmia (2013), http://dx.doi.org/10.1016/j.joa.2012.12.008

limited number of patients focused on lead aVR and defined "aVR sign" as R wave ≥ 0.3 mV or $R/q \geq 0.75$ in lead aVR [69]. Patients with aVR sign frequently had recurrent events during follow-up.

4.2. Fragmented QRS complex

Fragmented QRS (fQRS) is a convenient marker of ventricular conduction disturbance. It is usually evaluated by analyzing 12-lead ECGs and is defined as additional spikes within the QRS complex [70]. We defined the presence of fQRS in right bundle branch block (RBBB) as 1) ≥ 4 spikes in 1 or 2) ≥ 8 spikes in all of leads V1, V2, and V3 [71]. Only two control subjects with RBBB (2.5%) were regarded as having fQRS by this criterion. Patients with Brugada syndrome often had fQRS, and it was more frequently observed in the VF group (incidence of fQRS: VF 85%, syncope 50%, and asymptomatic 34%; $p < 0.01$) (Fig. 7). fQRS was not associated with the late potential (LP) recorded by a signal-averaged electrogram. Patients who had fQRS often experienced recurrent VF within 4 years of the first syncope or VF episodes.

Recently, the PRELUDE study has shown that fQRS was useful for identifying candidates for prophylactic ICD implantation (HR, 4.9), in addition to spontaneous type 1 ECG and a history of syncope as well as short ventricular refractory periods [4].

4.3. Prolongation of the PQ interval

Brugada et al. [1] in their initial report stated that patients with ACA had a longer HV interval. The PQ interval was usually normal, but patients with *SCN5A* mutation frequently had a longer PQ interval than did patients without an *SCN5A* mutation [72]. A recent study has shown that a long PQ interval (≥ 170 ms) was an independent risk factor for life-threatening events (OR, 11.5) [57].

4.4. Signal-averaged electrogram

In patients with Brugada syndrome, LPs are frequently detected by signal-averaged electrogram, especially in those with syncope or VF (incidences of LPs: 57–73% in total patients, 89–93% in patients with syncope, and 37–71% in asymptomatic patients) [51,73–75] and represent conduction disturbance of the RVOT area [76]. Patients with LPs often had induced VF [73] and showed daily fluctuation of the LPs [75]. A study showed that LPs are associated with subsequent cardiac events (HR, 10.9) [74].

5. Other indices

5.1. Prediction of outcome by electrophysiological study

The value of the inducibility of sustained ventricular arrhythmias during an electrophysiological study (EPS) for evaluating arrhythmic risk in Brugada syndrome is controversial [9,10]. Brugada et al. [2,7] showed that the inducibility of ventricular arrhythmias during an EPS was an independent predictor for cardiac events (HR, 8.33). However, other studies and a meta-analysis have failed to demonstrate its prognostic value [3–5,11,14,71].

VF induction by a small number of extrastimuli might indicate the existence of unstable arrhythmogenic substrate promoting VF. A recent study showed that the number of extrastimuli that induced VF served as a prognostic indicator for patients with type 1 ECG (HR, 3.21); however, the site of induction and the coupling interval that induced VF were not associated with cardiac events [77]. However, previous studies failed to show the prognostic value of the number of extrastimuli [4,14,35], and a prospective study with a large number of patients is required to prove the significance of the number of extrastimuli.

As parameters recorded during EPS, the significance of HV interval and ventricular refractory periods has been reported. The HV interval was prolonged in symptomatic patients but did not show a prognostic value [35]. Recently, a ventricular refractory period < 200 ms has been identified as an independent predictor of ventricular arrhythmias (HR, 3.91) [4].

5.2. Atrial arrhythmias

It is well known that patients with Brugada syndrome often have atrial arrhythmias, especially atrial fibrillation (AF) [78]. AF is an important cause of inappropriate discharge of an ICD in patients with Brugada syndrome [79]. The occurrence of AF is associated with cardiac events [79], and sometimes a new onset

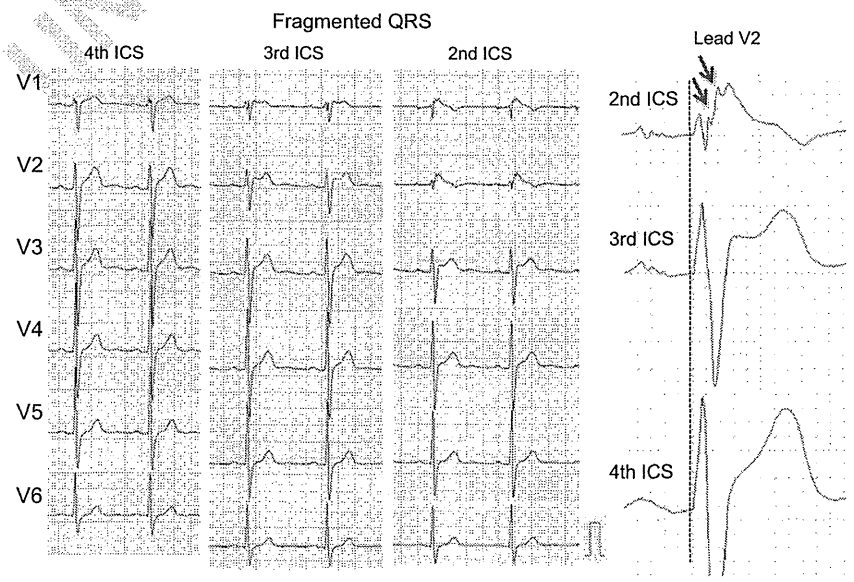

Fig. 7. Fragmented QRS. This patient with ventricular fibrillation (VF) had type 1 ECG and fragmented QRS in leads located at high intercostal spaces (ICSs). Arrows show multiple spikes within the QRS complex.

Please cite this article as: Wada T, Morita H. Clinical outcome and risk stratification in Brugada syndrome. J Arrhythmia (2013), http://dx.doi.org/10.1016/j.joa.2012.12.008

Table 3
Proposed risk stratification in Brugada syndrome.

Asymptomatic patients	Step 1	Spontaneous type 1 ECG (at any intercostal spaces)
	Step 2	VF induction by single or double extrastimuli ERP < 200 ms
	Step 3	Fragmented QRS Inferolateral ER Exercise-induced ST elevation
Patients with syncope	Step 1	Type 1 ECG (spontaneous or drug-induced)
	Step 2	Syncope without specific prodromes
	Step 3	VF induction by single or double extrastimuli ERP < 200 ms
	Step 4	Fragmented QRS Inferolateral ER Exercise-induced ST elevation
Additional observations		Family history of sudden death (< 45 years) PQ prolongation (≥ 170 ms) wide QRS complex (≥ 120 ms) T-wave alternans Spontaneous ST alteration (≥ 2 mm) ST augmentation by meal or full stomach Atrial fibrillation, sick sinus syndrome Late potential by SAECG

of AF precedes VF [80]. The occurrence of bradyarrhythmias is associated with high-risk patients [81]; however, it is not known whether AF and bradyarrhythmia can predict the development of VF during follow-up.

6. Summary and proposed risk stratification

The risk stratification of individuals without ACA is still controversial. As we have reviewed, many indices have been reported as prognostic predictors, but they are not always useful for identifying high-risk patients who do not have documented VF. In Japan, although most multicenter studies showed that patients with type 1 ECG were at high risk, it is difficult to determine whether implantation of an ICD should be preferred on the basis only of the ECG type.

The decision to implant an ICD in asymptomatic patients may be made by VF induction with a single or double extrastimuli in addition to the presence of spontaneous type 1 ECG [77]. The indication for an EPS is determined by the existence of ECG changes, including fQRS, inferolateral ER, and exercise-induced ST augmentation. If patients have one of these ECG findings, an EPS is recommended.

In patients with syncope episodes, detecting type 1 ECG (spontaneous or drug-induced) and evaluating the characteristics of symptoms are important for determining the indication for ICD implantation. The result of EPS is supportive; however, it should be noted that VF is not induced during EPS in all patients who have spontaneous VF episodes and that syncope is an important symptom preceding VF. The existence of fQRS, ER, and exercise-induced ST augmentation should also be considered (Table 3).

To determine the risk for patients, indices including family history and other various ECG markers are also considered in both asymptomatic patients and in those with syncope.

The incidence of a new onset of VF is not high in asymptomatic cases, and various clinical markers should be evaluated to identify high-risk patients in the future.

Conflict of interest

None.

Acknowledgments

This work was supported by a Grant-in-Aid for Scientific Research (C, 50322227) of Japan Society for the Promotion of Science (JSPS) and a research grant for cardiovascular diseases (H24-033) from the Ministry of Health, Labor, and Welfare of Japan.

References

[1] Brugada P, Brugada J. Right bundle branch block, persistent ST segment elevation and sudden cardiac death: a distinct clinical and electrocardiographic syndrome. A multicenter report. J Am Coll Cardiol 1992;20:1391–6.
[2] Brugada J, Brugada R, Antzelevitch C, et al. Long-term follow-up of individuals with the electrocardiographic pattern of right bundle-branch block and ST-segment elevation in precordial leads V1 to V3. Circulation 2002;105:73–8.
[3] Probst V, Veltmann C, Eckardt L, et al. Long-term prognosis of patients diagnosed with Brugada syndrome: Results from the FINGER Brugada syndrome registry. Circulation 2010;121:635–43.
[4] Priori SG, Gasparini M, Napolitano C, et al. Risk stratification in Brugada syndrome: results of the PRELUDE (PRogrammed ELectrical stimUlation preDictive valuE) registry. J Am Coll Cardiol 2012;59:37–45.
[5] Kamakura S, Ohe T, Nakazawa K, et al. Long-term prognosis of probands with Brugada-pattern ST-elevation in leads V1–V3. Circulat.: Arrhythmia Electrophysiol 2009;2:495–503.
[6] Brugada J, Brugada R, Brugada P. Right bundle-branch block and ST-segment elevation in leads V1 through V3: a marker for sudden death in patients without demonstrable structural heart disease. Circulation 1998;97:457–60.
[7] Brugada J, Brugada R, Brugada P. Determinants of sudden cardiac death in individuals with the electrocardiographic pattern of Brugada syndrome and no previous cardiac arrest. Circulation 2003;108:3092–6.
[8] Myerburg RJ, Marchlinski FE, Scheinman MM. Controversy on electrophysiology testing in patients with Brugada syndrome. Heart Rhythm 2011;8:1972–4.
[9] Brugada J, Brugada R, Brugada P. Electrophysiologic testing predicts events in Brugada syndrome patients. Heart Rhythm 2011;8:1595–7.
[10] Wilde AA, Viskin S. EP testing does not predict cardiac events in Brugada syndrome. Heart Rhythm 2011;8:1598–600.
[11] Gehi AK, Duong TD, Metz LD, et al. Risk stratification of individuals with the Brugada electrocardiogram: a meta-analysis. J Cardiovasc Electrophysiol 2006;17:577–83.
[12] Paul M, Gerss J, Schulze-Bahr E, et al. Role of programmed ventricular stimulation in patients with Brugada syndrome: a meta-analysis of worldwide published data. Eur Heart J 2007;28:2126–33.
[13] Antzelevitch C, Brugada P, Borggrefe M, et al. Brugada syndrome: report of the second consensus conference: endorsed by the Heart Rhythm Society and the European Heart Rhythm Association. Circulation 2005;111:659–70.
[14] Priori SG, Napolitano C, Gasparini M, et al. Natural history of Brugada syndrome: insights for risk stratification and management. Circulation 2002;105:1342–7.
[15] Roos M, Sarkozy A, Brodbeck J, et al. The importance of class-I antiarrhythmic drug test in the evaluation of patients with syncope: unmasking Brugada syndrome. J Cardiovasc Electrophysiol 2012;23:290–5.
[16] Raju H, Papadakis M, Govindan M, et al. Low prevalence of risk markers in cases of sudden death due to Brugada syndrome relevance to risk stratification in Brugada syndrome. J Am Coll Cardiol 2011;57:2340–5.
[17] Kubala M, Aissou L, Traulle S, et al. Use of implantable loop recorders in patients with Brugada syndrome and suspected risk of ventricular arrhythmia. Europace 2012;14:898–902.
[18] Yokokawa M, Okamura H, Noda T, et al. Neurally mediated syncope as a cause of syncope in patients with Brugada electrocardiogram. J Cardiovasc Electrophysiol 2010;21:186–92.
[19] Sacher F, Arsac F, Wilton SB, et al. Syncope in Brugada syndrome patients: prevalence, characteristics, and outcome. Heart Rhythm 2012;9:1272–9.
[20] Take Y, Morita H, Toh N, et al. Identification of high-risk syncope related to ventricular fibrillation in patients with Brugada syndrome. Heart Rhythm 2012;9:752–9.
[21] Sarkozy A, Sorgente A, Boussy T, et al. The value of a family history of sudden death in patients with diagnostic type I Brugada ECG pattern. Eur Heart J 2011;32:2153–60.
[22] Brugada P, Brugada R, Brugada J. Sudden death in high-risk family members: Brugada syndrome. Am J Cardiol 2000;86:40K–3K.
[23] Nishii N, Ogawa M, Morita H, et al. SCN5A mutation is associated with early and frequent recurrence of ventricular fibrillation in patients with Brugada syndrome. Circ J 2010;74:2572–8.
[24] Meregalli PG, Tan HL, Probst V, et al. Type of SCN5A mutation determines clinical severity and degree of conduction slowing in loss-of-function sodium channelopathies. Heart Rhythm 2009;6:341–8.
[25] Antzelevitch C. Genetic, molecular and cellular mechanisms underlying the J wave syndromes. Circ J 2012;76:1054–65.

Please cite this article as: Wada T, Morita H. Clinical outcome and risk stratification in Brugada syndrome. J Arrhythmia (2013), http://dx.doi.org/10.1016/j.joa.2012.12.008

[26] Eckardt L. Gender differences in Brugada syndrome. J Cardiovasc Electrophysiol 2007;18:422–4.
[27] Di Diego JM, Cordeiro JM, Goodrow RJ, et al. Ionic and cellular basis for the predominance of the Brugada syndrome phenotype in males. Circulation 2002;106:2004–11.
[28] Matsuo K, Akahoshi M, Seto S, Yano K. Disappearance of the Brugada-type electrocardiogram after surgical castration: a role for testosterone and an explanation for the male preponderance. Pacing and Clin Electrophysiol 2003;26:1551–3.
[29] Shimizu W, Matsuo K, Kokubo Y, et al. Sex hormone and gender difference—role of testosterone on male predominance in Brugada syndrome. J Cardiovasc Electrophysiol 2007;18:415–21.
[30] Benito B, Sarkozy A, Mont L, et al. Gender differences in clinical manifestations of Brugada syndrome. J Am Coll Cardiol 2008;52:1567–73.
[31] Brugada P, Benito B, Brugada R, et al. Brugada syndrome: update 2009. Hellenic J Cardiol 2009;50:352–72.
[32] Oe H, Takagi M, Tanaka A, et al. Prevalence and clinical course of the juveniles with Brugada-type ECG in Japanese population. Pacing Clin Electrophysiol 2005;28:549–54.
[33] Yamakawa Y, Ishikawa T, Uchino K, et al. Prevalence of right bundle-branch block and right precordial ST-segment elevation (Brugada-type electrocardiogram) in Japanese children. Circ J 2004;68:275–9.
[34] Probst V, Denjoy I, Meregalli PG, et al. Clinical aspects and prognosis of Brugada syndrome in children. Circulation 2007;115:2042–8.
[35] Brugada P, Brugada R, Mont L, et al. Natural history of Brugada syndrome: the prognostic value of programmed electrical stimulation of the heart. J Cardiovasc Electrophysiol 2003;14:455–7.
[36] Atarashi H, Ogawa S. New ECG criteria for high-risk Brugada syndrome. Circ J 2003;67:8–10.
[37] Hisamatsu K, Morita H, Fukushima Kusano K, et al. Evaluation of the usefulness of recording the ECG in the 3rd intercostal space and prevalence of Brugada-type ECG in accordance with recently established electrocardiographic criteria. Circ J 2004;68:135–8.
[38] Shimizu W, Matsuo K, Takagi M, et al. Body surface distribution and response to drugs of ST segment elevation in Brugada syndrome: clinical implication of eighty-seven-lead body surface potential mapping and its application to twelve-lead electrocardiograms. J Cardiovasc Electrophysiol 2000;11:396–404.
[39] Miyamoto K, Yokokawa M, Tanaka K, et al. Diagnostic and prognostic value of a type 1 Brugada electrocardiogram at higher (third or second) V1 to V2 recording in men with Brugada syndrome. Am J Cardiol 2007;99:53–7.
[40] Nagase S, Hiramatsu S, Morita H, et al. Electroanatomical correlation of repolarization abnormalities in Brugada syndrome: detection of type 1 electrocardiogram in the right ventricular outflow tract. J Am Coll Cardiol 2010;56:2143–5.
[41] Take Y, Morita H, Wu J, et al. Spontaneous electrocardiogram alterations predict ventricular fibrillation in Brugada syndrome. Heart Rhythm 2011;8:1014–21.
[42] Morita H, Zipes DP, Wu J. Brugada syndrome: insights of ST elevation, arrhythmogenicity, and risk stratification from experimental observations. Heart Rhythm 2009;6:S34–43.
[43] Evain S, Briec F, Kyndt F, et al. Sodium channel blocker tests allow a clear distinction of electrophysiological characteristics and prognosis in patients with a type 2 or 3 Brugada electrocardiogram pattern. Heart Rhythm 2008;5:1561–4.
[44] Chevallier S, Forclaz A, Tenkorang J, et al. New electrocardiographic criteria for discriminating between Brugada types 2 and 3 patterns and incomplete right bundle branch block. J Am Coll Cardiol 2011;58:2290–8.
[45] Morita H, Zipes DP, Lopshire J, et al. T wave alternans in an in vitro canine tissue model of Brugada syndrome. Am J Physiol: Heart Circ Physiol 2006;291:H421–8.
[46] Schulze-Bahr E, Zoelch KA, Eckardt L, et al. Electrical alternans in long QT syndrome resembling a Brugada syndrome pattern. Pacing Clin Electrophysiol 2003;26:2033–5.
[47] Morita H, Nagase S, Kusano K, et al. T. Spontaneous T wave alternans and premature ventricular contractions during febrile illness in a patient with Brugada syndrome. J Cardiovasc Electrophysiol 2002;13:816–8.
[48] Tada H, Nogami A, Shimizu W, et al. ST segment and T wave alternans in a patient with Brugada syndrome. Pacing Clin Electrophysiol 2000;23:413–5.
[49] Nishizaki M, Fujii H, Sakurada H, et al. Spontaneous T wave alternans in a patient with Brugada syndrome—responses to intravenous administration of class I antiarrhythmic drug, glucose tolerance test, and atrial pacing. J Cardiovasc Electrophysiol 2005;16:217–20.
[50] Morita H, Morita ST, Nagase S, et al. Ventricular arrhythmia induced by sodium channel blocker in patients with Brugada syndrome. J Am Coll Cardiol 2003;42:1624–31.
[51] Ikeda T, Sakurada H, Sakabe K, et al. Assessment of noninvasive markers in identifying patients at risk in the Brugada syndrome: insight into risk stratification. J Am Coll Cardiol 2001;37:1628–34.
[52] Matsuo K, Shimizu W, Kurita T, et al. Dynamic changes of 12-lead electrocardiograms in a patient with Brugada syndrome. J Cardiovasc Electrophysiol 1998;9:508–12.
[53] Veltmann C, Schimpf R, Echternach C, et al. A prospective study on spontaneous fluctuations between diagnostic and non-diagnostic ECGs in Brugada syndrome: implications for correct phenotyping and risk stratification. Eur Heart J 2006;27:2544–52.
[54] Richter S, Sarkozy A, Veltmann C, et al. Variability of the diagnostic ECG pattern in an ICD patient population with Brugada syndrome. J Cardiovasc Electrophysiol 2009;20:69–75.
[55] Castro Hevia J, Antzelevitch C, Tornes Barzaga F, et al. Tpeak–Tend and Tpeak–Tend dispersion as risk factors for ventricular tachycardia/ventricular fibrillation in patients with the Brugada syndrome. J Am Coll Cardiol 2006;47:1828–34.
[56] Sangawa M, Morita H, Nakatsu T, et al. Abnormal transmural repolarization process in patients with Brugada syndrome. Heart Rhythm 2009;6:1163–9.
[57] Miyamoto A, Hayashi H, Makiyama T, et al. Risk determinants in individuals with a spontaneous type 1 Brugada ECG. Circ J 2011;75:844–51.
[58] Makimoto H, Nakagawa E, Takaki H, et al. Augmented ST-segment elevation during recovery from exercise predicts cardiac events in patients with Brugada syndrome. J Am Coll Cardiol 2010;56:1576–84.
[59] Nishizaki M, Sakurada H, Ashikaga T, et al. Effects of glucose-induced insulin secretion on ST segment elevation in the Brugada syndrome. J Cardiovasc Electrophysiol 2003;14:243–9.
[60] Nishizaki M, Sakurada H, Mizusawa Y, et al. Influence of meals on variations of ST segment elevation in patients with Brugada syndrome. J Cardiovasc Electrophysiol 2008;19:62–8.
[61] Nogami A, Nakao M, Kubota S, et al. Enhancement of J-ST-segment elevation by the glucose and insulin test in Brugada syndrome. Pacing Clin Electrophysiol 2003;26:332–7.
[62] Ikeda T, Abe A, Yusu S, et al. The full stomach test as a novel diagnostic technique for identifying patients at risk of Brugada syndrome. J Cardiovasc Electrophysiol 2006;17:602–7.
[63] Haissaguerre M, Derval N, Sacher F, et al. Sudden cardiac arrest associated with early repolarization. N Eng J Med 2008;358:2016–23.
[64] Letsas KP, Sacher F, Probst V, et al. Prevalence of early repolarization pattern in inferolateral leads in patients with Brugada syndrome. Heart Rhythm 2008;5:1685–9.
[65] Sarkozy A, Chierchia GB, Paparella G, et al. Inferior and lateral electrocardiographic repolarization abnormalities in Brugada syndrome. Circulat: Arrhythmia Electrophysiol 2009;2:154–61.
[66] Kawata H, Noda T, Yamada Y, et al. Effect of sodium-channel blockade on early repolarization in inferior/lateral leads in patients with idiopathic ventricular fibrillation and Brugada syndrome. Heart Rhythm 2012;9:77–83.
[67] Takagi M, Yokoyama Y, Aonuma K, et al. Clinical characteristics and risk stratification in symptomatic and asymptomatic patients with Brugada syndrome: multicenter study in Japan. J Cardiovasc Electrophysiol 2007;18:1244–51.
[68] Junttila MJ, Brugada P, Hong K, et al. Differences in 12-lead electrocardiogram between symptomatic and asymptomatic Brugada syndrome patients. J Cardiovasc Electrophysiol 2008;19:380–3.
[69] Babai Bigi MA, Aslani A, Shahrzad S. aVR sign as a risk factor for life-threatening arrhythmic events in patients with Brugada syndrome. Heart Rhythm 2007;4:1009–12.
[70] Das MK, Saha C, El Masry H, et al. Fragmented QRS on a 12-lead ECG: a predictor of mortality and cardiac events in patients with coronary artery disease. Heart Rhythm 2007;4:1385–92.
[71] Morita H, Kusano KF, Miura D, et al. Fragmented QRS as a marker of conduction abnormality and a predictor of prognosis of Brugada syndrome. Circulation 2008;118:1697–704.
[72] Yokokawa M, Noda T, Okamura H, et al. Comparison of long-term follow-up of electrocardiographic features in Brugada syndrome between the SCN5A-positive probands and the SCN5A-negative probands. Am J Cardiol 2007;100:649–55.
[73] Morita H, Takenaka-Morita S, Fukushima-Kusano K, et al. Risk stratification for asymptomatic patients with Brugada syndrome. Circ J 2003;67:312–6.
[74] Huang Z, Patel C, Li W, et al. Role of signal-averaged electrocardiograms in arrhythmic risk stratification of patients with Brugada syndrome: a prospective study. Heart Rhythm 2009;6:1156–62.
[75] Tatsumi H, Takagi M, Nakagawa E, et al. Risk stratification in patients with Brugada syndrome: analysis of daily fluctuations in 12-lead electrocardiogram (ECG) and signal-averaged electrocardiogram (SAECG). J Cardiovasc Electrophysiol 2006;17:705–11.
[76] Hisamatsu K, Kusano KF, Morita H, et al. Relationships between depolarization abnormality and repolarization abnormality in patients with Brugada syndrome: using body surface signal-averaged electrocardiography and body surface maps. J Cardiovasc Electrophysiol 2004;15:870–6.
[77] Makimoto H, Kamakura S, Aihara N, et al. Clinical impact of the number of extrastimuli in programmed electrical stimulation in patients with Brugada type 1 electrocardiogram. Heart Rhythm 2012;9:242–8.
[78] Morita H, Kusano-Fukushima K, Nagase S, et al. Atrial fibrillation and atrial vulnerability in patients with Brugada syndrome. J Am Coll Cardiol 2002;40:1437–44.
[79] Bordachar P, Reuter S, Garrigue S, et al. Incidence, clinical implications and prognosis of atrial arrhythmias in Brugada syndrome. Eur Heart J 2004;25:879–84.
[80] Pappone C, Radinovic A, Manguso F, et al. New-onset atrial fibrillation as first clinical manifestation of latent Brugada syndrome: prevalence and clinical significance. Eur Heart J 2009;30:2985–92.
[81] Makiyama T, Akao M, Tsuji K, et al. High risk for bradyarrhythmic complications in patients with Brugada syndrome caused by SCN5A gene mutations. J Am Coll Cardiol 2005;46:2100–6.

Please cite this article as: Wada T, Morita H. Clinical outcome and risk stratification in Brugada syndrome. J Arrhythmia (2013), http://dx.doi.org/10.1016/j.joa.2012.12.008

Circulation Journal
Official Journal of the Japanese Circulation Society
http://www.j-circ.or.jp

ORIGINAL ARTICLE
Regenerative Medicine

Ultrastructural Maturation of Human-Induced Pluripotent Stem Cell-Derived Cardiomyocytes in a Long-Term Culture

Tsukasa Kamakura, MD; Takeru Makiyama, MD, PhD; Kenichi Sasaki, MD; Yoshinori Yoshida, MD, PhD; Yimin Wuriyanghai; Jiarong Chen; Tetsuhisa Hattori, MD, PhD; Seiko Ohno, MD, PhD; Toru Kita, MD, PhD; Minoru Horie, MD, PhD; Shinya Yamanaka, MD, PhD; Takeshi Kimura, MD, PhD

Background: In the short- to mid-term, cardiomyocytes generated from human-induced pluripotent stem cells (hiPSC-CMs) have been reported to be less mature than those of adult hearts. However, the maturation process in a long-term culture remains unknown.

Methods and Results: A hiPSC clone generated from a healthy control was differentiated into CMs through embryoid body (EB) formation. The ultrastructural characteristics and gene expressions of spontaneously contracting EBs were analyzed through 1-year of culture after cardiac differentiation was initiated. The 14-day-old EBs contained a low number of myofibrils, which lacked alignment, and immature high-density Z-bands lacking A-, H-, I-, and M-bands. Through the long-term culture up to 180 days, the myofibrils became more tightly packed and formed parallel arrays accompanied by the appearance of mature Z-, A-, H-, and I-bands, but not M-bands. Notably, M-bands were finally detected in 360-day-old EBs. The expression levels of the M-band-specific genes in hiPSC-CMs remained lower in comparison with those in the adult heart. Immunocytochemistry indicated increasing number of MLC2v-positive/MLC2a-negative cells with decreasing number of MLC2v/MLC2a double-positive cells, indicating maturing of ventricular-type CMs.

Conclusions: The structural maturation process of hiPSC-CMs through 1-year of culture revealed ultrastructural sarcomeric changes accompanied by delayed formation of M-bands. Our study provides new insight into the maturation process of hiPSC-CMs. (*Circ J* 2013; **77:** 1307–1314)

Key Words: Cardiomyocytes; Induced pluripotent stem cells; Ultrastructure

Induced pluripotent stem cells (iPSC) can differentiate into functional cardiomyocytes (CMs), and are a powerful model for regenerative therapy and investigating the mechanisms underlying inherited cardiac diseases.[1–5] Although several studies have shown that iPSC-derived CMs (iPSC-CMs) have molecular, structural and functional properties resembling those of adult CMs,[6–9] they have proved to be less mature than adult and fetal CMs.[10–12] Thus, there is limited information about the electrophysiological and biochemical properties of iPSC-CMs, and the ultrastructural maturation process has not been investigated fully.

The ultrastructural features of human iPSC-CMs (hiPSC-CMs) at around 30 days after cardiac differentiation have been described as being similar to those of adult CMs showing myofibrillar bundles with transverse Z-bands.[4,13,14] However, in those reports, hiPSC-CMs still remain embryonic in phenotype, lacking a mature sarcomeric structure with M-bands and a variable degree of myofibrillar organization. It is unknown whether hiPSC-CMs can develop the adult CM-like ultrastructure in vitro. Immaturity of the hiPSC-CMs may hamper their application for studying cardiac diseases, drug development, and regenerative medicine, and could affect functional properties and drug responses in vitro and increase the risk of abnormal growth in vivo. Therefore, it is crucial to elucidate the

Received July 31, 2012; revised manuscript received December 7, 2012; accepted January 8, 2013; released online February 9, 2013 Time for primary review: 27 days

Department of Cardiovascular Medicine, Kyoto University Graduate School of Medicine, Kyoto (T. Kamakura, T.M., K.S., Y.W., J.C., T. Kimura); Department of Cardiovascular and Respiratory Medicine, Shiga University of Medical Science, Otsu (T.H., S.O., M.H.); Center for iPS Cell Research and Application (CiRA), Institute for Integrated Cell-Material Sciences Kyoto University, Kyoto (Y.Y., S.Y.); and Department of Cardiovascular Medicine, Kobe City General Hospital, Kobe (T. Kita), Japan

Mailing addresses: Takeru Makiyama, MD, PhD, Department of Cardiovascular Medicine, Kyoto University Graduate School of Medicine, 54 Kawahara-cho, Shogoin, Sakyo-ku, Kyoto 606-8507, Japan. E-mail: makiyama@kuhp.kyoto-u.ac.jp and Yoshinori Yoshida, MD, PhD, Center for iPS Cell Research and Application (CiRA), Institute for Integrated Cell-Material Sciences, Kyoto University, 53 Kawahara-cho, Shogoin, Sakyo-ku, Kyoto 606-8507, Japan. E-mail: yoshinor@cira.kyoto-u.ac.jp

ISSN-1346-9843 doi:10.1253/circj.CJ-12-0987

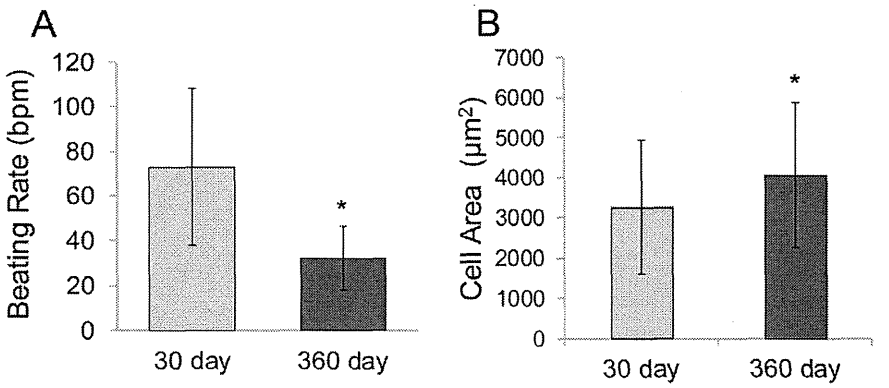

Figure 1. Comparison of human-induced pluripotent stem cell-derived cardiomyocytes (hiPSC-CMs) at 30 and 360 days after cardiac differentiation. (**A**) The rate of beating (beats/min [bpm]) of embryoid bodies (EBs) at 30 days was significantly higher than that of 360-day EBs (73.2±34.9 bpm vs. 32.2±14.2 bpm, P<0.0001). (**B**) Size of hiPSC-CMs increased significantly after long-term culture (3,277.4±1,679.5 μm^2 vs. 4,067.9±1,814.6 μm^2, P=0.01). *P<0.05 vs. 30-day.

maturation process and establish a protocol for creating homogeneous mature iPSC-CMs.

In this study, we investigated the ultrastructural, immunocytological, and gene expression changes of hiPSC-CMs in a long-term 2D culture. Here, we first report that mature sarcomeric structures with M-bands were detected only in 360-day hiPSC-CMs, which might be associated with lower expression levels of M-band-specific proteins compared with adult heart cells.

Methods

Culture of hiPSC and CM Differentiation

The hiPSC line 201B7 was retrovirally transfected with Oct3/4, SOX-2, Klf4, and c-Myc.[1,9] These lines displayed all the defining parameters[1] and the hiPSCs were maintained as described.[15]

We differentiated hiPSC-CMs as embryoid bodies (EBs).[16,17] In brief, hiPSCs aggregated to form EBs, and were cultured in suspension for 8 days. On day 8, the EBs were plated onto fibronectin-coated dishes and for the first 20 days, we followed the protocol as described previously.[16,17] Cultures were maintained in a 5% CO_2, 5% O_2, 90% N_2 environment for the first 12 days and then transferred into a 5% CO_2/air environment for the remainder of the culture period. At 20 days after cardiac differentiation, EBs were maintained in culture DMEM/F12 supplemented with 2% fetal bovine serum, 2 mmol/L L-glutamine, 0.1 mmol/L non-essential amino acids, 0.1 mmol/L β-mercaptoethanol, 50 U/ml penicillin, and 50 μg/ml streptomycin.[3] The medium was renewed every 2–3 days.

Immunocytochemistry

For immunostaining, single cells were isolated from microdissected 30- and 360-day-old beating EBs using collagenase B (Roche) and trypsin EDTA (Nacalai Tesque). The cells were plated onto fibronectin-coated dishes for 3 days to allow attachment. The cells were fixed in 4% paraformaldehyde and permeabilized in 0.2% Triton X-100 (Nacalai Tesque). The samples were stained with the following primary antibodies: rabbit polyclonal anti-cardiac troponin I (cTnI) (1:200; Santa Cruz), mouse monoclonal anti-myosin light chain 2a (MLC2a) (1:200; Synaptic Systems), rabbit polyclonal anti-myosin light chain 2v (MLC2v) (1:100; Proteintech Group), mouse monoclonal anti-βIII tubulin (1:100, Promega), mouse monoclonal anti-fibroblast (1:100, Acris Antibodies), and mouse monoclonal anti-human smooth muscle actin (1:100, Dako). We used the appropriate secondary antibodies: donkey anti-rabbit Alexafluor 594 (1:500, Invitrogen) and donkey anti-mouse Alexafluor 488 (1:500, Invitrogen). The nuclei were stained with DAPI (1:2000, Wako). The specimens were observed under a fluorescence microscope, Biozero BZ-9000 (Keyence), and the areas of cTnI-positive cells were calculated using a BZ-II analyzer (Keyence).

Transmission Electron Microscopy (TEM)

TEM was performed on 14-, 30-, 60-, 90-, 180-, and 360-day old EBs derived from hiPSC-CMs. EBs were microdissected and fixed for 1 h in 2% glutaraldehyde at 4°C in phosphate-buffered saline (PBS). All sections were treated with OsO_4 (1% for 1 min, and 0.5% for 20 min at 4°C) in PBS, dehydrated in ethanol and propylene oxide, and embedded in Luveak 812 (Nacalai Tesque). Ultrathin sections were cut with an ultramicrotome (Leica, Heidelberg, Germany) and observed with TEM (H-7650; Hitachi). All stages of EBs were examined in triplicate.

Analysis of mRNA Expression by Real-Time Quantitative Polymerase Chain Reaction (qPCR)

Total RNA was isolated using TRIzol Reagent (Invitrogen) from 20 to 30 EBs microdissected from 30-, 90-, 180-, and 360-day-old hiPSC-CMs, and treated with TURBO DNA-free Kit (Applied Biosystems). Total RNA from human heart tissue (left ventricle, left atrium, and fetal heart) was also reverse transcribed into complementary DNA (cDNA) for comparison. cDNA was synthesized from 1 μg of total RNA, in a total volume of 20 μl, using oligo $(dT)_{18}$ primer with Transcriptor First Strand cDNA Synthesis Kit (Roche). The PCR-related primers are detailed in **Table S1**. The real-time qPCR was performed using power SYBR Green PCR Master Mix (Applied Biosystems) for 6 samples. The expression of genes of interest was normalized to that of *GAPDH*. Relative quantification was calculated according to the $\Delta\Delta C_T$ method. The changes in gene expression levels were compared with those of hiPSC-

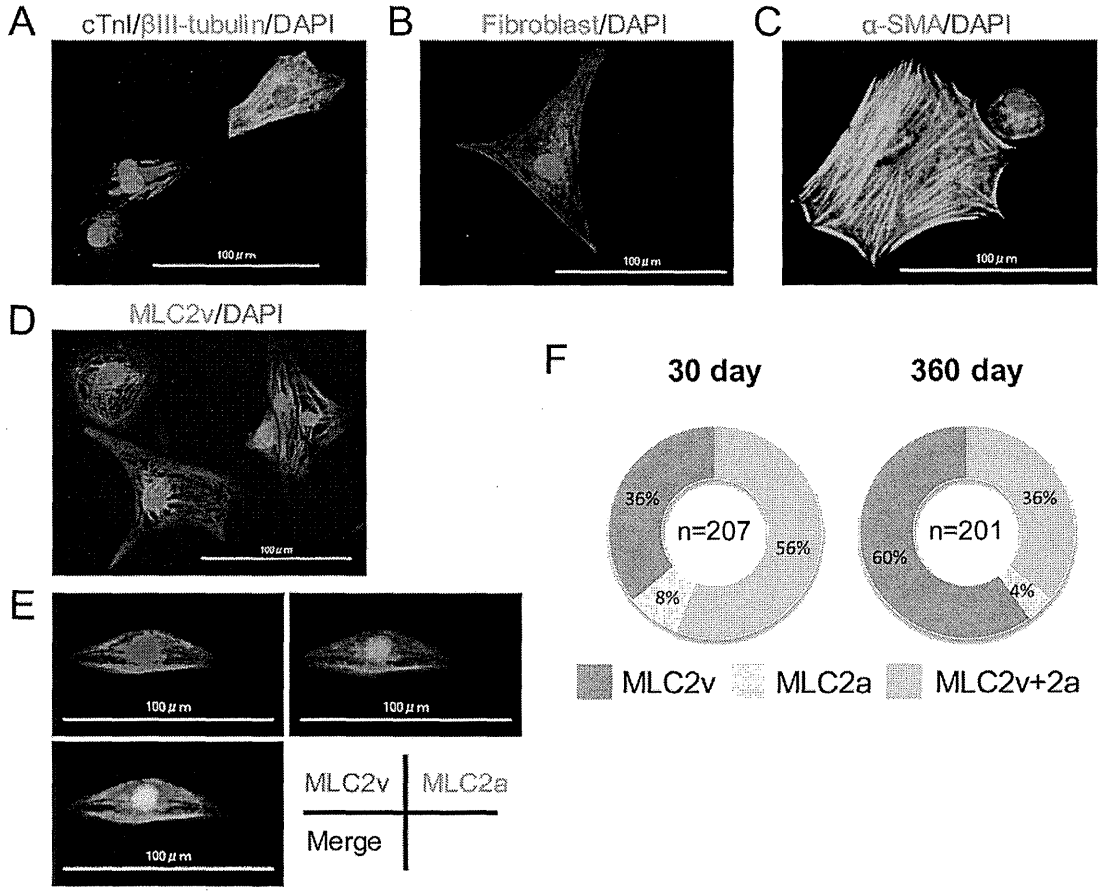

Figure 2. Immunostaining of human-induced pluripotent stem cell-derived cardiomyocytes (hiPSC-CMs) at 30 days after cardiac differentiation. (**A–E**) Immunostaining of single cells isolated from microdissected beating embryoid bodies (EBs) at 30 days using the following antibodies: (**A**) cTnI (red), βIII-tublin (green), and DAPI (blue); (**B**) fibroblast (green) and DAPI (blue); (**C**) α-SMA (green) and DAPI (blue); (**D**) MLC2v (green) and DAPI (blue); (**E**) MLC2v (red) and MLC2a (green). (**E**) hiPSC-CM expressing both MLC2v and MLC2a. (**F**) Properties of MLC2v-positive/MLC2a-negative, MLC2v-negative/MLC2a-positive, and MLC2v/MLC2a double-positive cells at 30 days and 360 days. Among the MLC2v- or MLC2a-positive cells, 36% of 30-day hiPSC-CMs were MLC2v-positive/MLC2a-negative mature ventricular CMs and 56% were MLC2v/MLC2a double-positive immature ventricular CMs. At day 360, MLC2v-positive/MLC2a-negative mature CMs increased to 60%, whereas MLC2v/MLC2a double-positive immature ventricular CMs decreased to 36%.

CMs at 30-day differentiation. The fold change is expressed as mean±SEM.

Statistical Analysis

All values are presented as mean±SEM. Statistical significance was evaluated by Student's t-test for 2 groups or 1-way analysis of variance followed by Tukey test for comparisons of multiple groups. Differences with $P<0.05$ were considered statistically significant.

Results

Long-Term Maintenance of hiPSC-CMs

Areas of spontaneous beating became visible as early as day 8 after differentiation, and kept beating for more than 360 days (**Movie S1**). The beating rate of 30-day-old EBs (n=42) was significantly higher than that of 360-day-old EBs (n=41; 73.2± 34.9 beats/min vs. 32.2±14.2 beats/min, $P<0.0001$) (**Figure 1A**).

The size of dispersed hiPSC-CMs increased significantly after long-term culture as measured by their cell area (3,277.4± 1,679.5 μm^2 vs. 4,067.9±1,814.6 μm^2, $P=0.01$) (**Figure 1B**).

Immunostaining Analysis of Beating EBs at 30 and 360 Days After Cardiac Differentiation

Immunostaining of single cells isolated by microdissected beating EBs detected cells positive not only for cTnI, MLC2v, and MLC2a, but also βIII-tubulin, fibroblasts, and α-SMA, suggesting the existence of neural cells, fibroblast-like cells, and vascular smooth muscle cells in the beating EBs as well as CMs (**Figures 2A–E**).

Among randomly selected single cells isolated from 30- (n=213) and 360-day-old (n=191) beating EBs, 61% and 64%, respectively, were positive for cTnI. Double immunostaining with anti-MLC2v and anti-MLC2a antibodies revealed that among the MLC2v- or MLC2a-positive cells, 36% were MLC2v-positive/MLC2a-negative, 8% were MLC2v-negative/

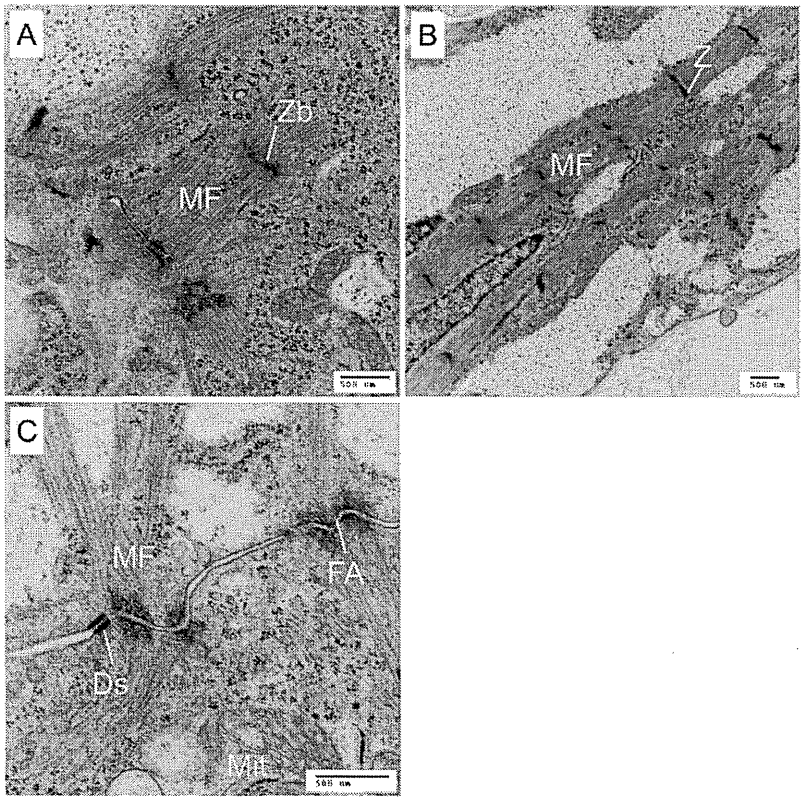

Figure 3. Transmission electron microscopy images of human-induced pluripotent stem cell-derived cardiomyocytes (hiPSC-CMs) at 14 days after cardiac differentiation. (**A**) hiPSC-CMs at 14 days contained myofibrils (MF) that lacked alignment or organized sarcomeric pattern. Scattered condensed Z-bodies (Zb) were also confirmed. (**B**) In some areas, a more developed pattern was noted in which myofibrils (MF) were held between a few of the Z-bands (Z). (**C**) CMs connected by desmosomes (Ds) and fascia adherens (FA) even at this early stage. Mitochondria (Mit) can be seen.

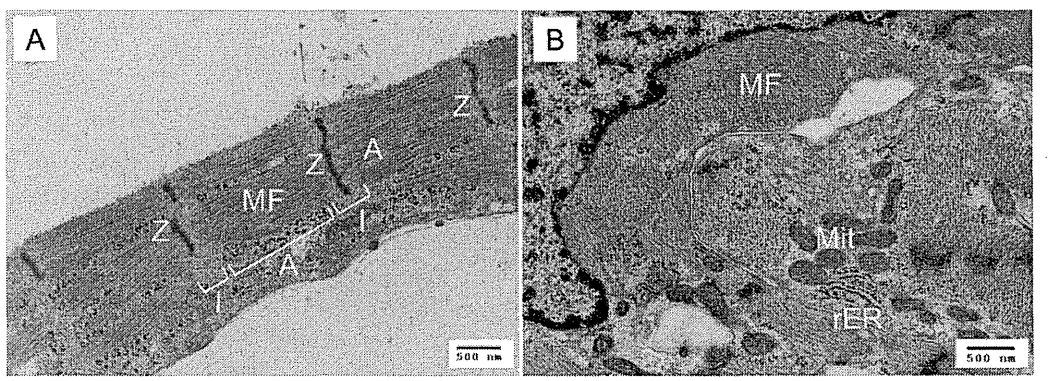

Figure 4. Transmission electron microscopy images of human-induced pluripotent stem cell-derived cardiomyocytes (hiPSC-CMs) at 30 days after cardiac differentiation. (**A**) hiPSC-CMs at 30 days appeared to be packed between parallel Z-bands. Some myofibrils (MF) showed A- (A) and I-bands (I). (**B**) Transverse section of sarcomere and rough endoplasmic reticulum (rER). Mitochondria (Mit) can be seen.

MLC2a-positive, and 56% were MLC2v/MLC2a double-positive CMs at 30-day differentiation. By day 360, MLC2v-positive/MLC2a-negative CMs increased to 60%, whereas MLC2v/MLC2a double-positive immature ventricular CMs decreased to 36% (**Figure 2F**).

Ultrastructural Analysis of hiPSC-CMs at 14-, 30-, 60-, 90-, 180-, and 360-Day Differentiation

hiPSC-CMs at 14-day differentiation contained myofibrils that lacked alignment or organized sarcomeric pattern, and were distributed diffusely in the cytoplasm in a disorganized fashion. Scattered patterns of condensed Z-bodies were also confirmed. However, in some areas, a more developed pattern was

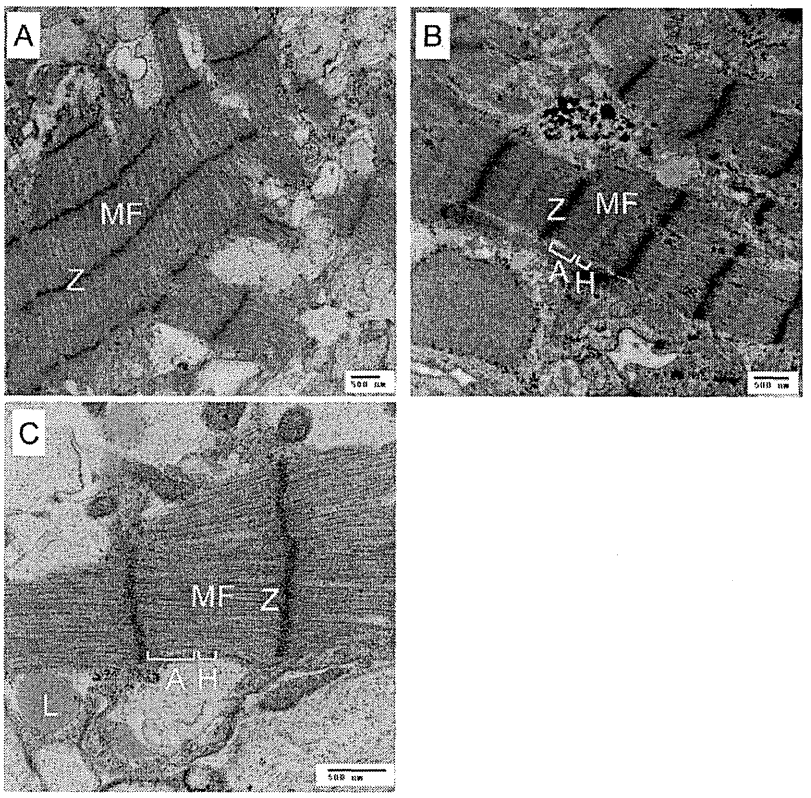

Figure 5. Transmission electron microscopy images of human-induced pluripotent stem cell-derived cardiomyocytes (hiPSC-CMs) at 60 (**A**), 90 (**B**), and 180 days (**C**) after cardiac differentiation. Between 60- and 180-day differentiation, ultrastructural maturation continued and formation of H-bands (H) can be seen. However, even at 180-day differentiation, M-bands are not apparent. Lipid droplets (L) can be seen in (**C**).

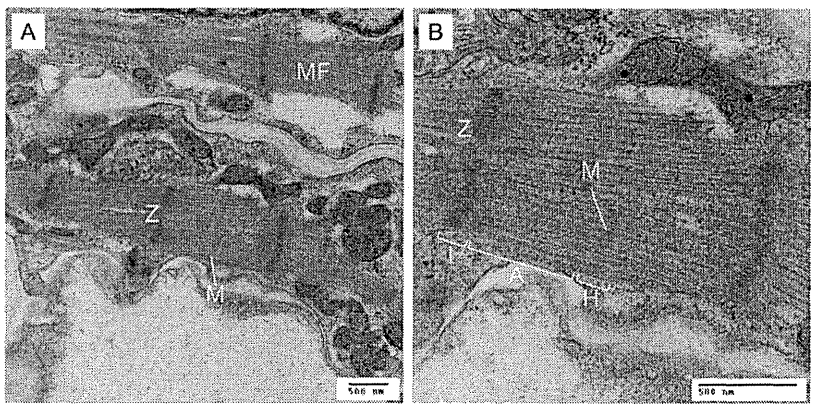

Figure 6. Transmission electron microscopy images of human-induced pluripotent stem cell-derived cardiomyocytes (hiPSC-CMs) at 360 days after cardiac differentiation. (**A**,**B**) In addition to discrete A-, H-, I-, and Z-bands, M-bands (M) are also noted in a minority of the cells within the sarcomeres.

noted in which myofibrils were held between a few of the Z-bands (**Figure 3**). However, A-, H-, I-, and M-bands were not recognized. CMs were connected by desmosomes and fascia adherens at this early stage.

At 30-day differentiation, nascent myofibrils decreased and appeared to be packed between Z-bands. Parallel Z-bands were demonstrated to confine the myofibrils in the typical sarcomeric pattern. Some myofibrils showed A- and I-bands. However, they still lacked the formation of H-, and M-bands (**Figure 4**). Mitochondria and rough endoplasmic reticulum were also noted, as previously reported.[13]

Between 60- and 90-day differentiation, ultrastructural maturation continued and formation of H-bands could be observed. However, even at 180-day differentiation, M-bands could not be detected (**Figure 5**).

Finally, at 360-day differentiation, in addition to discrete A-, H-, I-, and Z-bands, M-bands were first noted in a minority of the cells within the sarcomeres (**Figure 6**). Myofibrils appeared to be tightly packed and distributed in an oriented fashion. The amount of sarcomeric structure in a single CM continued to increase, but was still scarce compared with an adult CM. Even at this stage, different degrees of organization

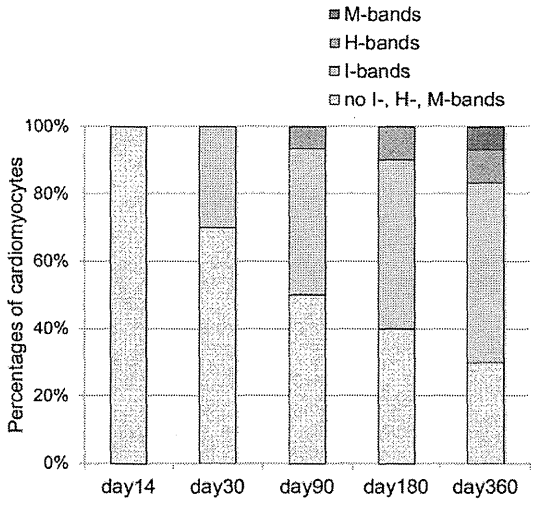

Figure 7. Percentages of the cardiomyocytes (CMs) having I-, H-, and M-bands at 14, 30, 90, 180, 360 days after cardiac differentiation. The amount of CMs with I- and H-bands increased through the long-term culture and M-bands were first noted in 360-day CMs.

existed simultaneously in the same EB.

We evaluated 30 CMs with sarcomeres on randomly selected electron micrographs to assess the maturation process of sarcomeres quantitatively. **Figure 7** shows the percentages of CMs having I-, H-, and M-bands at 14-, 30-, 90-, 180-, 360-day differentiation.

Expression of Cardiac-Specific Genes

Leucine-rich repeat-containing protein 39 (*LRRC39*), myomesin 1 (*MYOM1*), and 2 (*MYOM2*), components of M-bands,[18] increased at 360-day differentiation compared with 30-day differentiation, supporting the observation of M-band formation in 360-day hiPSC-CMs (**Figure 8**). However, the expression levels of the M-band-specific proteins in the hiPSC-CMs were lower compared with those of the adult heart. The expression of cardiac troponin-T (*cTnT*), myosin heavy chain 6 (*MYH6*), myosin heavy chain 7 (*MYH7*), and myosin regulatory light chain 2 (*MYL2*) also increased after the 1-year culture. However, the expression levels of cardiac-specific genes in the hiPSC-CMs were also considerably lower than those in the adult heart left ventricle or left atrium, and in the fetal heart. The expression levels of gap junction α-1 protein were significantly decreased in 180-day and 360-day hiPSC-CMs compared with 30-day hiPSC-CMs.

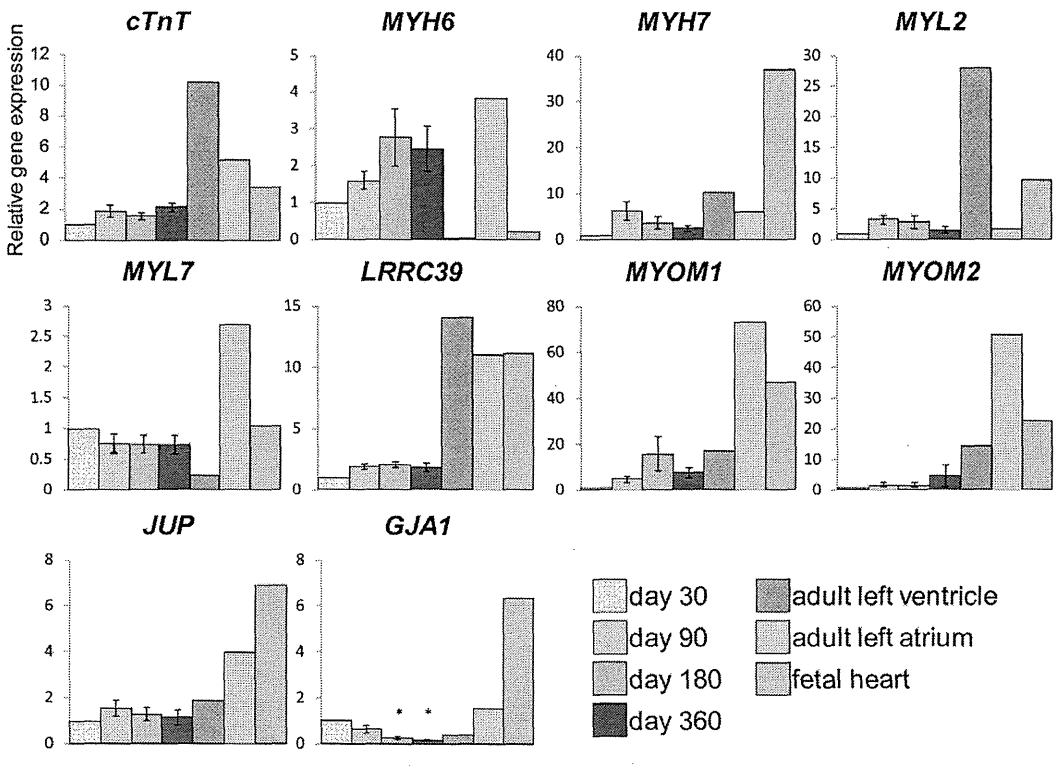

Figure 8. Real-time quantitative polymerase chain reaction analyses for *cTnT*, *MYH6*, *MYH7*, *MYL2*, *MYL7*, *LRRC39*, *MYOM1*, *MYOM2*, *JUP*, and *GJA1* expression in beating embryoid bodies (EB) from human-induced pluripotent stem cell-derived cardiomyocytes (hiPSC-CMs) at 30, 90, 180, and 360 days, in the adult left ventricle, adult left atrium, and fetal heart. The changes in gene expression levels were compared with those of hiPSC-CMs at 30-day differentiation. *cTnT*, cardiac troponin-T; *MYH6*, myosin heavy chain 6; *MYH7*, myosin heavy chain 7; *MYL2*, myosin regulatory light chain 2; *MYL7*, myosin regulatory light chain 7; *LRRC39*, leucine-rich repeat-containing protein 39; *MYOM1*, myomesin 1; *MYOM2*, myomesin 2; *JUP*, junction plakoglobin; *GJA1*, gap junction α-1 protein. *P<0.05 vs. 30-days EBs.

Discussion

In this study, we demonstrated that hiPSC-CMs continue to mature through a 1-year culture. This is the first report of the feasibility of 1-year 2D culture of hiPSC-CMs and description of the sarcomeric maturation process represented by the emergence of M-bands and the increase in the cardiac-specific gene expressions.

So far, the reported ultrastructure of hiPSC-CMs has been immature and their maturation process remained unknown.[4,13,14] Human embryonic stem cell-derived cardiomyocytes (hESC-CMs) are reported to follow a roughly similar maturation process to that reported both in vivo and in an in-vitro murine ES model.[19–24] The hiPSC-CMs in the present study showed a similar maturation process to that of hESC-CMs.[25] At first, narrow, diffusely distributed, and frequently not well aligned myofibrils, resembling those of hiPSC-CMs at 14 days, developed into sarcomeres with clear band patterns including the Z-, I-, and A-bands, responding to hiPSC-CMs at between 30 and 90 days, and ultimately resulted in the generation of well-designed sarcomeres with A-, H-, I-, and M-bands. The ultrastructural findings of hiPSC-CMs in the literature now available relate to around 30 days of differentiation, and only Z- and I-bands have been visible.[4,13,14] In our study, the 30-day hiPSC-CMs similarly showed only Z- and I-bands, not H- or M-bands. Notably, we are the first to find that only 360-day hiPSC-CMs, not 180-day hiPSC-CMs, show a mature sarcomeric structure with M-bands. However, even at 360-day differentiation, different degrees of organization patterns existed simultaneously in the same EB and homogeneous maturation was not confirmed. Our 1-year culture system was able to confirm more mature sarcomeric structures than previously reported, but still not that of adult CMs. It is reported that human CMs derived from fetal hearts do not achieve full ultrastructural maturity and that myofibrillar development continues throughout the entire fetal period.[22] The insufficient maturation of hiPSC-CMs after long-term culture could be explained by several factors. In vitro culturing conditions lack the presence of adjacent non-myocyte proliferating cells, which play an important role in the maturation of CMs via paracrine and humoral signals in vivo. In addition, the CMs grown in the absence of hemodynamic workload typical of in vivo working CMs are reported to lack appropriate ultrastructural development.[26] The differences between in vitro and in vivo conditions, such as the absence of humoral factors and organized mechanical and electrical stress in vitro, might result in delayed ultrastructural maturation.

In electron micrographs of the sarcomere, the M-band appears as a series of parallel electron-dense lines in the central zone of the A-band. The M-band has been reported to play a role not only in mechanical stability in the activated sarcomere, such as reducing the intrinsic instability of thick filaments and helping titin to maintain order in sarcomeres, but also in the biomechanical conditions in contracting muscle such as stress sensing.[27] M-band formation was confirmed in the latest stage and has been considered the endpoint of myofibrillar maturation.[18,21] The lower expression levels of the M-band-specific proteins in the hiPSC-CMs compared with the adult heart might be associated with the delayed appearance of M-bands. Maturation of iPSC-CMs is critical for their application in regenerative medicine, as well as for investigating the mechanisms underlying inherited cardiac diseases. Techniques to promote the maturation of ESC-CMs, such as 3D culture methodology,[28] electric stimulation,[29] and coculture with non-cardiomyocytes[30] may be applicable to iPSC-CMs to overcome the problem, although it has not been fully investigated in hiPSC-CMs. Improved methods are needed to produce homogeneous, mature iPSC-CMs.

In addition to ultrastructural maturation, there was a significant increase in the size of hiPSC-CMs after long-term culture, supporting the process of morphological maturation. Also, the lower rate of beating of 360-day hiPSC-CMs compared with 30-day hiPSC-CMs suggested electrophysiological maturation, because it has been reported that the resting membrane potential becomes progressively more negative in the developing atrial and ventricular myocytes, which correlates with an increasing presence of I_{K1}, and ultimately, the fetal atrial and ventricular myocytes exhibit stable resting membrane potentials with little automaticity.[31]

Changes in the expression patterns of MLC2v and MLC2a occur during the maturation process.[32] hiPSC-CMs were thought to be immature and similar to human fetal CMs because of the presence of a number of MLC2v/MLC2a double-positive CMs.[33] Our immunostaining analysis demonstrated that the percentage of MLC2v/MLC2a double-positive hiPSC-CMs decreased after long-term culture, accompanied by an increase in MLC2v-positive/MLC2a-negative hiPSC-CMs, suggesting maturing of the ventricular-type CMs.

This study also showed for the first time, changes in the expression levels of cardiac-specific genes and genes related to intercalated discs throughout the 1-year culture. The cardiac-specific genes tended to increase during 1-year culture, supporting the maturation process of hiPSC-CMs. The connexin (gap junction proteins) are reported to be more abundant in the neonate than the adult.[34] The significant decrease in *GJA1* expression levels in 180- and 360-day hiPSC-CMs compared with 30-day hiPSC-CMs also suggested maturation of hiPSC-CMs.

Study Limitations

We used microdissected beating EBs for the gene expression studies. The fact that EBs contain CMs at various stages of differentiation, as well as non-CMs, might obscure the results of the gene expression studies. We conducted immunostaining analysis of single cells from microdissected beating EBs 3 days after enzymatic dispersion, which might allow non-CMs to increase and affect the results of the percentage of CMs in the beating EBs.

Conclusions

The current study demonstrated developmental changes in the ultrastructural, immunocytological, and gene expression properties of hiPSC-CMs. Our results confirmed mature sarcomeric structure with M-band formation in long-term culture of hiPSC-CMs for the first time, which provides a new insight into the maturation process of hiPSC-CMs. For application of homogeneous mature hiPSC-CMs in regenerative medicine and in vitro modeling of human cardiac diseases, further maturation of cardiac cells will be needed.

Acknowledgments

We thank Aya Umehara, Masako Tanaka, Kyoko Yoshida, and the Division of Electron Microscopic Study, Center for Anatomical Studies, Kyoto University Graduate School of Medicine for technical assistance.

Sources of Funding

This work was supported by research grants from the Ministry of Education, Culture, Science, and Technology of Japan (T.M. and M.H.), Suzuken Memorial Foundation (T. Kimura), Fujiwara Memorial Foundation

(T.M.), the Uehara Memorial Foundation (M.H.), and health science research grants from the Ministry of Health, Labor and Welfare of Japan for Clinical Research on Measures for Intractable Diseases (T.M. and M.H.).

Disclosures

None.

References

1. Takahashi K, Tanabe K, Ohnuki M, Narita M, Ichisaka T, Tomoda K, et al. Induction of pluripotent stem cells from adult human fibroblasts by defined factors. *Cell* 2007; **131:** 861–872.
2. Zhang J, Wilson GF, Soerens AG, Koonce CH, Yu J, Palecek SP, et al. Functional cardiomyocytes derived from human-induced pluripotent stem cells. *Circ Res* 2009; **104:** e30–e41.
3. Moretti A, Bellin M, Welling A, Jung CB, Lam JT, Bott-Flügel L, et al. Patient-specific induced pluripotent stem-cell models for long-QT syndrome. *N Engl J Med* 2010; **363:** 1397–1409.
4. Novak A, Barad L, Zeevi-Levin N, Shick R, Shtrichman R, Lorber A, et al. Cardiomyocytes generated from $CPVT^{D307H}$ patients are arrhythmogenic in response to β-adrenergic stimulation. *J Cell Mol Med* 2012; **16:** 468–482.
5. Choi SH, Jung SY, Kwon SM, Baek SH. Perspectives on stem cell therapy for cardiac regeneration. *Circ J* 2012; **76:** 1307–1312.
6. Zwi L, Caspi O, Arbel G, Huber I, Gepstein A, Park IH, et al. Cardiomyocyte differentiation of human-induced pluripotent stem cells. *Circulation* 2009; **120:** 1513–1523.
7. Germanguz I, Sedan O, Zeevi-Levin N, Shtrichman R, Barak E, Ziskind A, et al. Molecular characterization and functional properties of cardiomyocytes derived from human inducible pluripotent stem cells. *J Cell Mol Med* 2011; **14:** 38–51.
8. Ma J, Guo L, Fiene SJ, Anson BD, Thomson JA, Kamp TJ, et al. High purity human-induced pluripotent stem cell-derived cardiomyocytes electrophysiological properties of action potentials and ionic currents. *Am J Physiol Heart Circ Physiol* 2011; **301:** H2006–H2017.
9. Tanaka T, Tohyama S, Murata M, Nomura F, Kaneko T, Chen H, et al. In vitro pharmacologic testing using human-induced pluripotent stem cell-derived cardiomyocytes. *Biochem Biophys Res Commun* 2009; **385:** 497–502.
10. Xi J, Khalil M, Shishechian N, Hannes T, Pfannkuche K, Liang H, et al. Comparison of contractile behavior of native murine ventricular tissue and cardiomyocytes derived from embryonic or induced pluripotent stem cells. *FASEB J* 2010; **24:** 2739–2751.
11. Kuzmenkin A, Liang H, Xu G, Pfannkuche K, Eichhorn H, Fatima A, et al. Functional characterization of cardiomyocytes derived from murine induced pluripotent stem cells in vitro. *FASEB J* 2009; **23:** 4168–4180.
12. Jonsson MK, Vos MA, Mirams GR, Duker G, Sartipy P, de Boer TP, et al. Application of human stem cell-derived cardiomyocytes in safety pharmacology requires caution beyond hERG. *J Mol Cell Cardiol* 2012; **52:** 998–1008.
13. Gherghiceanu M, Barad L, Novak A, Reiter I, Itskovitz-Eldor J, Binah O, et al. Cardiomyocytes derived from human embryonic and induced pluripotent stem cells: Comparative ultrastructure. *J Cell Mol Med* 2011; **15:** 2539–2551.
14. Fujiwara M, Yan P, Otsuji TG, Narazaki G, Uosaki H, Fukushima H, et al. Induction and enhancement of cardiac cell differentiation from mouse and human-induced pluripotent stem cells with cyclosporine-A. *PLoS One* 2011; **6:** e16734.
15. Yoshida Y, Takahashi K, Okita K, Ichisaka T, Yamanaka S. Hypoxia enhances the generation of induced pluripotent stem cells. *Cell Stem Cell* 2009; **5:** 237–241.
16. Dubois NC, Craft AM, Sharma P, Elliott DA, Stanley EG, Elefanty AG, et al. SIRPA is a specific cell-surface marker for isolating cardiomyocytes derived from human pluripotent stem cells. *Nat Biotechnol* 2011; **29:** 1011–1018.
17. Yang L, Soonpaa MH, Adler ED, Roepke TK, Kattman SJ, Kennedy M, et al. Human cardiovascular progenitor cells develop from a KDR^+ embryonic-stem-cell-derived population. *Nature* 2008; **453:** 524–528.
18. Will RD, Eden M, Just S, Hansen A, Eder A, Frank D, et al. Myomasp/LRRC39, a heart- and muscle-specific protein, is a novel component of the sarcomeric M-band and is involved in stretch sensing. *Circ Res* 2010; **107:** 1253–1264.
19. Beharvand H, Azarnia M, Parivar K, Ashtiani SK. The effect of extracellular matrix on embryonic stem cell-derived cardiomyocytes. *J Mol Cel Cardiol* 2005; **38:** 495–503.
20. Baharvand H, Piryaei A, Rohani R, Taei A, Heidari MH, Hosseini A. Ultrastructural comparison of developing mouse embryonic stem cell- and in vivo-derived cardiomyocytes. *Cell Biol Int* 2006; **30:** 800–807.
21. Anversa P, Olivetti G, Bracchi PG, Loud AV. Postnatal development of the M-band in rat cardiac myofibrils. *Circ Res* 1981; **48:** 561–568.
22. Kim HD, Kim DJ, Lee IJ, Rah BJ, Sawa Y, Schaper J. Human fetal heart development after mid-term: Morphometry and ultrastructural study. *J Mol Cell Cardiol* 1992; **24:** 949–965.
23. Legat MJ. Sarcomerogenesis in human myocardium. *J Mol Cell Cardiol* 1970; **1:** 425–437.
24. Yu L, Gao S, Nie L, Tang M, Huang W, Luo H, et al. Molecular and functional changes in voltage-gated Na^+ channels in cardiomyocytes during mouse embryogenesis. *Circ J* 2011; **75:** 2071–2079.
25. Snir M, Kehat I, Gepstein A, Coleman R, Itskovitz-Eldor J, Livne E, et al. Assessment of the ultrastructural and proliferative properties of human embryonic stem cell-derived cardiomyocytes. *Am J Physiol Heart Circ Physiol* 2003; **285:** H2355–H2363.
26. Bishop SP, Anderson PG, and Tucker DC. Morphological development of the rat heart growing in oculo in the absence of hemodynamic work load. *Circ Res* 1990; **66:** 84–102.
27. Agarkova I, Perriard JC. The M-band: An elastic web that crosslinks thick filaments in the center of the sarcomere. *Trends Cell Biol* 2005; **15:** 477–485.
28. Ou DB, He Y, Chen R, Teng JW, Wang HT, Zeng D, et al. Three-dimensional co-culture facilitates the differentiation of embryonic stem cells into mature cardiomyocytes. *J Cell Biochem* 2011; **112:** 3555–3562.
29. Chen MQ, Xie X, Wilson KD, Sun N, Wu JC, Giovangrandi L, et al. Current-controlled electrical point-source stimulation of embryonic stem cells. *Cell Mol Bioeng* 2009; **2:** 625–635.
30. Kim C, Majdi M, Xia P, Wei KA, Talantova M, Spiering S, et al. Non-cardiomyocytes influence the electrophysiological maturation of human embryonic stem cell-derived cardiomyocytes during differentiation. *Stem Cells Dev* 2010; **19:** 783–795.
31. He JQ, Ma Y, Lee Y, Thomson JA, Kamp TJ. Human embryonic stem cells develop into multiple types of cardiac myocytes: Action potential characterization. *Circ Res* 2003; **93:** 32–39.
32. Kubalak SW, Miller-Hance WC, O'Brien TX, Dyson E, Chien KR. Chamber specification of atrial myosin light chain-2 expression precedes septation during murine cardiogenesis. *J Biol Chem* 1994; **269:** 16961–16970.
33. Mummery CL, Zhang J, Ng ES, Elliott DA, Elefanty AG, Kamp TJ. Differentiation of human embryonic stem cells and induced pluripotent stem cells to cardiomyocytes: A methods overview. *Circ Res* 2012; **111:** 344–358.
34. Allah EA, Tellez JO, Yanni J, Nelson T, Monfredi O, Boyett MR, et al. Changes in the expression of ion channels, connexins and Ca^{2+}-handling proteins in the sino-atrial node during postnatal development. *Exp Physiol* 2011; **96:** 426–438.

Supplementary Files

Supplementary File 1

Table S1. Primer Sequences Used for Real-Time qPCR Analysis

Supplementary File 2

Movie S1. 360-day-old beating embryoid bodies.

Please find supplementary file(s);
http://dx.doi.org/10.1253/circj.CJ-12-0987

A novel mutation in the transmembrane nonpore region of the *KCNH2* gene causes severe clinical manifestations of long QT syndrome

Li Liu, MD,* Kenshi Hayashi, MD, PhD,† Tomoya Kaneda, MD, PhD,‡ Hidekazu Ino, MD, PhD,† Noboru Fujino, MD, PhD,† Katsuharu Uchiyama, MD, PhD,† Tetsuo Konno, MD, PhD,† Toyonobu Tsuda, MD,† Masa-aki Kawashiri, MD, PhD,† Kosei Ueda, MD, PhD,‡ Toshinori Higashikata, MD, PhD,‡ Wen Shuai, MS,§ Sabina Kupershmidt, PhD,§ Haruhiro Higashida, MD, PhD,* Masakazu Yamagishi, MD, PhD†

*From the *Department of Biophysical Genetics, Kanazawa University Graduate School of Medical Science, Kanazawa, Japan, †Division of Cardiovascular Medicine, Kanazawa University Graduate School of Medical Science, Kanazawa, Japan, ‡Komatsu Municipal Hospital, Komatsu, Japan and §Anesthesiology Research Division, Vanderbilt University School of Medicine, Nashville, Tennessee.*

BACKGROUND Long QT syndrome (LQTS) is characterized by prolonged ventricular repolarization and variable clinical course with arrhythmia-related syncope and sudden death. Mutations in the nonpore region of the LQTS-associated *KCNH2* gene (also known as hERG) are mostly associated with coassembly or trafficking abnormalities, resulting in haplotype insufficiency and milder clinical phenotypes compared with mutations in the pore domain.

OBJECTIVE To investigate the effect of a nonpore mutation on the channel current, which was identified from an LQTS family with severe clinical phenotypes.

METHODS Two members of a Japanese family with LQTS were searched for mutations in *KCNQ1, KCNH2, SCN5A, KCNE1, KCNE2,* and *KCNJ2* genes by using automated DNA sequencing. We characterized the electrophysiological properties and glycosylation pattern of the mutant channels by using patch clamp recording and Western blot analysis.

RESULTS In the LQTS patient with torsades de pointes and cardiopulmonary arrest, we identified the novel T473P mutation in the transmembrane nonpore region of *KCNH2*. The proband's father carried the same mutation and showed prolonged corrected QT interval and frequent torsades de pointes in the presence of hypokalemia following the administration of garenoxacin. Patch clamp analysis in heterologous cells showed that hERG T473P channels generated no current and exhibited a dominant negative effect when coexpressed with wild-type protein. Only incompletely glycosylated hERG T473P channels were observed by using Western blot analysis, suggesting impaired trafficking.

CONCLUSIONS These results demonstrated that a trafficking-deficient mutation in the transmembrane nonpore region of *KCNH2* causes a dominant negative effect and a severe clinical course in affected patients.

KEYWORDS Long QT syndrome; *KCNH2*; Nonpore region; Trafficking deficient; Dominant negative

ABBREVIATIONS ECG = electrocardiogram; I_{Kr} = delayed rectifier K^+ current; **LQT2** = long QT syndrome type 2; **LQTS** = long QT syndrome; **QTc** = corrected QT; **TdP** = torsades de pointes

(Heart Rhythm 2013;10:61–67)

Introduction

Long QT syndrome (LQTS) is characterized by prolonged ventricular repolarization and malignant arrhythmia leading to syncope, cardiac arrest, and sudden death.[1] Genetic studies have so far identified 13 forms of congenital LQTS caused by mutations in genes of cardiac ion channels or ion channel modulators, including membrane adapters.[2] The acquired form of LQTS is more common than the congenital form; risk factors include drugs administered for noncardiac conditions, over-the-counter drugs, hypokalemia, bradycardia, and genetic variations in ion channel genes.[3]

The *KCNH2* gene encodes the Kv11.1 protein α subunit (hERG) that underlies the rapidly activating delayed rectifier K^+ current (I_{Kr}) in the heart, which is active during phases 2 and 3 of the cardiac action potential and plays an important role in cardiac repolarization. Mutations in *KCNH2* are responsible for LQTS type 2 (LQT2), and many mutations or polymorphisms in this gene have been identified in patients with both congenital and acquired LQTS.[4–7] Previous studies showed

The first 3 authors contributed equally to this work. This study was supported in part by grants from the Ministry of Health, Labour and Welfare of Japan. **Address reprint requests and correspondence:** Kenshi Hayashi, MD, PhD, Division of Cardiovascular Medicine, Kanazawa University Graduate School of Medical Science, 13-1, Takara-machi, Kanazawa, Ishikawa 920-8640, Japan. E-mail address: kenshi@med.kanazawa-u.ac.jp.

1547-5271/$-see front matter http://dx.doi.org/10.1016/j.hrthm.2012.09.053